

4

AFGL-TR-88-0263  
ENVIRONMENTAL RESEARCH PAPERS, NO. 1013

## Effects of Low Flying Aircraft on Archaeological Structures

JAMES C. BATTIS

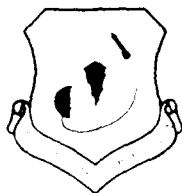
AD-A215 447



26 September 1988



Approved for public release; distribution unlimited.



EARTH SCIENCES DIVISION

PROJECT 7600

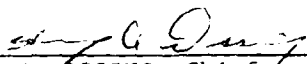
**AIR FORCE GEOPHYSICS LABORATORY**

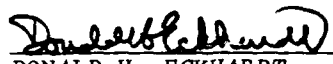
HANSCOM AFB, MA 01731

89 12 18 127

"This Technical Report has been reviewed and is approved for publication."

FOR THE COMMANDER

  
HENRY A. OSSING, Chief  
Solid Earth Geophysics Branch

  
DONALD H. ECKHARDT  
Director  
Earth Sciences Division

This report has been reviewed by the ESD Public Affairs Office (PA) and is releasable to the National Technical Information Service (NTIS).

Qualified requestors may obtain additional copies from the Defense Technical Information Center. All others should apply to the National Technical Information Service.

If your address has changed, or if you wish to be removed from the mailing list, or if the addressee is no longer employed by your organization, please notify GL/IMA, Hanscom AFB, MA 01731. This will assist us in maintaining a current mailing list.

Do not return copies of this report unless contractual obligations or notices on a specific document requires that it be returned.

UNCLASSIFIED

SECURITY CLASSIFICATION OF THIS PAGE

REPORT DOCUMENTATION PAGE				Form Approved OMB No. 0704-0188	
1a. REPORT SECURITY CLASSIFICATION Unclassified			1b. RESTRICTIVE MARKINGS		
2a. SECURITY CLASSIFICATION AUTHORITY			3. DISTRIBUTION / AVAILABILITY OF REPORT Approved for public release; distribution unlimited		
2b. DECLASSIFICATION / DOWNGRADING SCHEDULE					
4. PERFORMING ORGANIZATION REPORT NUMBER(S) AFGL-TR-88-0263      EPR, No. 1013			5. MONITORING ORGANIZATION REPORT NUMBER(S)		
6a. NAME OF PERFORMING ORGANIZATION Air Force Geophysics Laboratory		6b. OFFICE SYMBOL (If applicable) LWH		7a. NAME OF MONITORING ORGANIZATION	
6c. ADDRESS (City, State, and ZIP Code) Hanscom AFB Massachusetts 01731-5000			7b. ADDRESS (City, State, and ZIP Code)		
8a. NAME OF FUNDING / SPONSORING ORGANIZATION		8b. OFFICE SYMBOL (If applicable)		9. PROCUREMENT INSTRUMENT IDENTIFICATION NUMBER	
8c. ADDRESS (City, State, and ZIP Code)		10. SOURCE OF FUNDING NUMBERS			
		PROGRAM ELEMENT NO. 62101F		PROJECT NO. 7600	TASK NO. 760009
				WORK UNIT ACCESSION NO. 76000308	
11. TITLE (Include Security Classification) Effects of Low Flying Aircraft on Archaeological Structures					
12. PERSONAL AUTHOR(S) Battis, J.C.					
13a. TYPE OF REPORT Scientific, Interim		13b. TIME COVERED FROM 1 Oct 87 TO 19 Sep 88		14. DATE OF REPORT (Year, Month, Day) 1988 September 26	
				15. PAGE COUNT 56	
16. SUPPLEMENTARY NOTATION					
17. COSATI CODES			18. SUBJECT TERMS (Continue on reverse if necessary and identify by block number)  Motion Forecasts, Cliff Dwellings, Long House		
FIELD	GROUP	SUB-GROUP			
19. ABSTRACT (Continue on reverse if necessary and identify by block number)  Induced vibrations from aircraft overflights were measured at Long House, an Anasazi Indian site dating from approximately AD 1300. Aircraft overflights were performed by RF-4C, A-7, and B-52 aircraft at altitudes ranging from 60 to over 300 meters AGL. Seismometers on the Long House structure recorded the site response. None of the overflights produced site responses exceeding established criteria for archaeological sites, taken to be a peak vector sum wall velocity of 1.3 mm/sec.					
20. DISTRIBUTION/AVAILABILITY OF ABSTRACT <input checked="" type="checkbox"/> UNCLASSIFIED/UNLIMITED <input type="checkbox"/> SAME AS RPT <input type="checkbox"/> DTIC USERS				21. ABSTRACT SECURITY CLASSIFICATION Unclassified	
22a. NAME OF RESPONSIBLE INDIVIDUAL James C. Battis				22b. TELEPHONE (Include Area Code) (617) 377-4870	
				22c. OFFICE SYMBOL AFGL/LWH	

DD FORM 1473, JUN 86

Previous editions are obsolete.

SECURITY CLASSIFICATION OF THIS PAGE:

UNCLASSIFIED

## Contents

1. INTRODUCTION	1
2. THE SITE	1
3. INSTRUMENTATION	3
4. VIBRATION CRITERIA	8
5. AIRCRAFT OVERFLIGHTS	8
5.1 B-52 Pressure Signatures	8
5.2 RF-4C and A-7 Pressure Signals	17
6. LONG HOUSE OVERFLIGHT RESPONSES	17
6.1 B-52 Overflight Responses	22
6.2 RF-4C and A-7 Overflight Responses	22
7. WALL ADMITTANCES	33
7.1 Overflight Admittances	33
7.2 Shotgun Admittances	46
8. RESULT SUMMARY	46
REFERENCES	49

Accession For	
NTIS GRA&I	<input checked="" type="checkbox"/>
DTIC TAB	<input checked="" type="checkbox"/>
Unannounced	<input type="checkbox"/>
Justification	
By	
Distribution/	
Availability Codes	
Mail and/or	
Dist	Special
A-1	

## Illustrations

1. Location of the Long House Site	2
2. Plan View of Long House Ruins Showing the Instrument Locations	4
3. Typical Instrument Response Function for a Dyneer S-6000 Seismometer Recorded Through a DCS-302 Field Recorder	6
4. Typical Instrument Response Function for a DJ Instruments Differential Pressure Transducer Recorded Through a DCS-302 Field Recorder	7
5. Typical Pressure Time History of a B-52 Overflight as Recorded at the Long House Site (Pass 6)	11
6. Spectral Estimate of the Pressure Background Noise Just Prior to B-52 Pass 6. (Aircraft at a range of 6000 meters)	13
7. Spectral Estimate of the Pressure Signal for B-52 Overflight 6 on Approach to Long House (Aircraft at a range of 600 meters)	14
8. Spectral Estimate of the Pressure Signal for B-52 Overflight 6 Overhead	15
9. Spectral Estimate of the Pressure Signal for B-52 Overflight 6 Departing from the Long House Sites (Aircraft at a Range of 600 meters)	16
10. Long Wall Segment Response for B-52 Overflight 6	23
11. Short Wall Segment Response for B-52 Overflight 6	24
12. Maximum Entropy Spectral Estimates of the Wall Motions at Site 2, the Long Wall Segment, During B-52 Overflight 6	
(a) Component of motion is N42E	25
(b) Component of motion is N48W	26
13. Maximum Entropy Spectral Estimates of the Wall Motions at Site 5, the Long Wall Segment, During B-52 Overflight 6	
(a) Component of motion is N42E	27
(b) Component of motion is N48W	28

## Illustrations

14. Long Wall Segment Maximum Response for RF-4C Overflight 3	29
15. Short Wall Maximum Response for RF-4C Overflight 5	30
16. Long Wall Segment Maximum Response for A-7 Overflight 9	31
17. Short Wall Maximum Response for A-7 Overflight 16	32
18. Maximum Entropy Spectral Estimates of the Wall Motions at Site 2, the Long Wall Segment, During RF-4C Overflight 3	
(a) Component of motion is N42E	34
(b) Component of motion is N48W	35
19. Maximum Entropy Spectral Estimates of the Wall Motions at Site 5, the Short Wall Segment, During RF-4C Overflight 5	
(a) Component of motion is N42E	36
(b) Component of motion is N48W	37
20. Maximum Entropy Spectral Estimates of the Wall Motions at Site 2, the Long Wall Segment, During A-7 Overflight 9	
(a) Component of motion is N42E	38
(b) Component of motion is N48W	39
21. Maximum Entropy Spectral Estimates of the Wall Motions at Site 5, the Short Wall Segment, During A-7 Overflight 16	
(a) Component of motion is N42E	40
(b) Component of motion is N48W	41
22. Long Wall Segment Admittance Function Based on B-52 Overflight Data	
(a) Component of motion is N42E	42
(b) Component of motion is N48W	43
23. Short Wall Segment Admittance Function Based on B-52 Overflight Data	
(a) Component of motion is N42E	44
(b) Component of motion is N48W	45
24. Long Wall Segment Admittance Function Based on Shotgun Blasts	
(a) Component of motion is N42E	47
(b) Component of motion is N48W	48

# Effects of Low-Flying Aircraft on Archaeological Structures

## 1. INTRODUCTION

The Air Force Strategic Air Command (SAC) maintains various low altitude training routes throughout the U.S. for the use of the bomber forces. In these routes SAC aircraft are authorized to fly as low as 120 m above ground level (AGL) to simulate combat operations. Many of the existing or potential routes in the southwestern U.S. pass over or are close to archaeological sites such as cliff dwellings or other ancient structures.

Questions have recently been raised on the potential threat posed to these sites by the low altitude aircraft operations. In response to those questions, the Air Force, in cooperation with the Navajo Nation began a study of this problem. Participating in these studies, in addition to AFGL, were the Historic Preservation Office of the Navajo Nation, Oak Ridge National Laboratory, the Air Force Noise and Sonic Boom Impact Technology Office and Air Force Civil Engineering Services Center. This report presents the results of the Air Force Geophysics Laboratory contribution to this effort, specifically the results obtained from direct observation of aircraft overflights at one particular site, Long House, near Kayenta, Arizona.

## 2. THE SITE

The Long House site is located approximately 20 km southwest of Kayenta, Arizona, as shown in Figure 1. The Long House ruins were part of an extensive Anasazi agricultural community that was

---

(Received for Publication 22 September 1988)

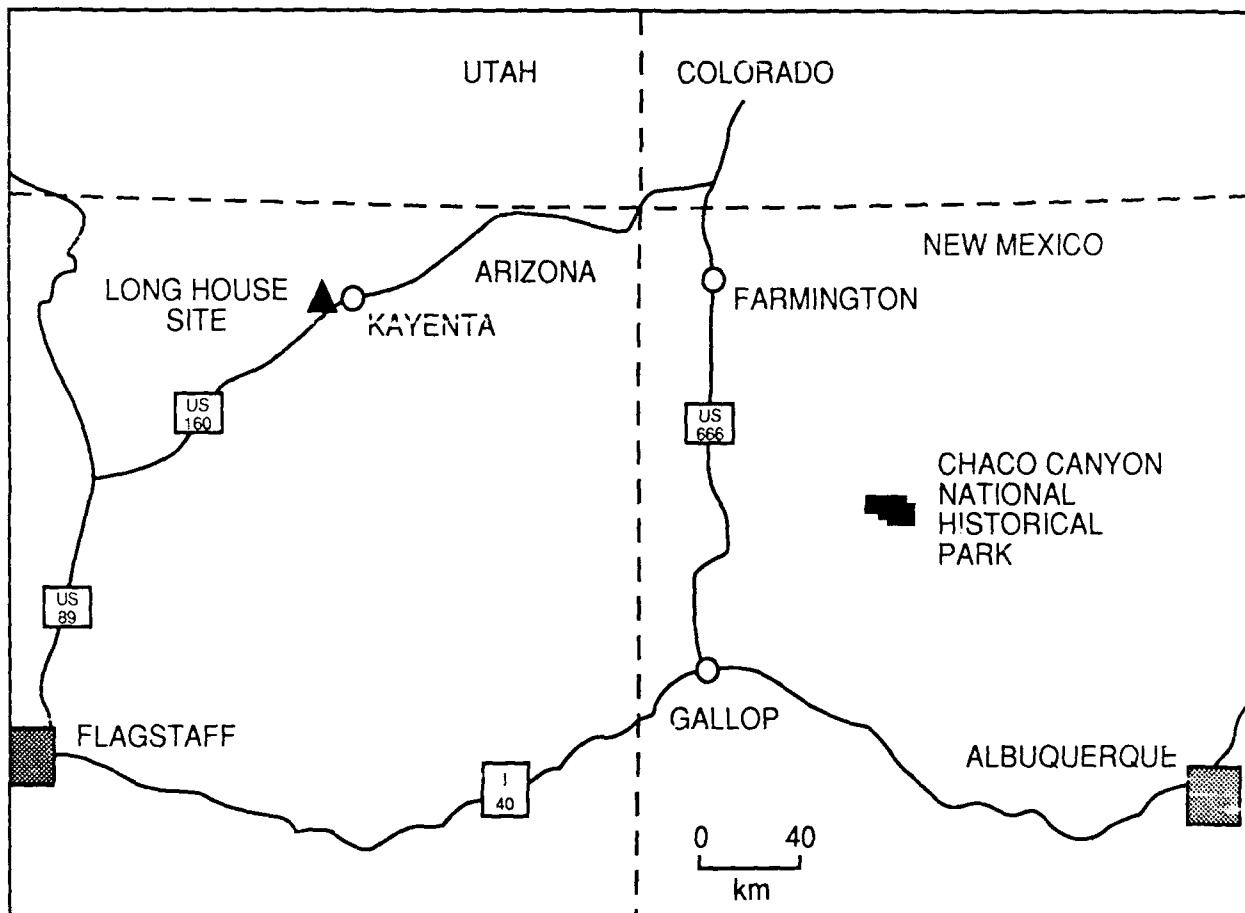


Figure 1. Location of the Long House Site



active between AD 1000 to 1300.<sup>1</sup> Long House itself was built very near AD 1274 on a small baldrock outcrop on the western side of Long House Valley. The standing ruins of Long House consist of two parallel walls, running northwest to southeast, and separated by approximately 3 meters (Figure 2). Each wall is survived by two segments, one of about 3 to 6 meters in length and one of about 15 to 20 meters. Both segments have a maximum height of approximately 3 meters. The walls are constructed of sandstone block facings with an adobe and stone rubble core and are approximately 0.7 - 0.8 meter thick.<sup>1</sup>

### 3. INSTRUMENTATION

Aircraft overflights were monitored at two locations at the Long House site to represent the motions of a short and long wall segments (Figure 2). Each location consisted of two Dyneer S-6000 triaxial seismometers, one at the top and one at the bottom of the wall, and three DJ instruments +/- 3.5 kPa differential pressure transducers. The three pressure transducers were essentially collocated near the base of the wall at each site.

The long wall site instruments were located approximately 5 meters from the end of a 15 meter long wall section. The instruments at the top of the wall were 2.2 meters above the ground level. The wall thickness for this section was estimated to average between 0.70 and 0.75 meter. The short wall segment had a length at the foundation level of 3.7 meters. Ground level between the walls of Long House was approximately 0.75 meter higher than outside, where the instruments were located. The wall was 3.0 meters high using the exterior measurement. The top seismometers were placed at a point 1.8 meters above the exterior ground level.

All seismometers were oriented with respect to the natural axes of the standing walls. One channel was oriented along the axis of the wall, N42E, a second was oriented normal to the axis of the wall, N48W, and the third was vertical. As will be shown it can be anticipated that the maximum motions would be on N48W data channels and that significantly smaller levels of motion would be observed on the vertical traces.

The transducer outputs were recorded on Terra Technology DCS-302 three channel digital data recorders. The DCS 302 units were operated at 100 samples per second, with one recorder for pressure transducers at 200 samples per second and provide automatic gain ranging over amplifications of 1000X, 250X, 50X or 10X the input voltage. Anti-alias filtering is performed by a 5th order Butterworth filter with a corner at 30 Hz for the 100 sample per second recorders and 70 Hz for the 200 sample per second recorder. The amplifications of these recorders have been found to be accurate within several percent of specification and, when no recent unit calibration is available, the nominal values can be used.

Transducer calibrations are given in Table 1 and were obtained *in-situ* for the seismometers. The pressure transducers were calibrated in the laboratory prior to the field experiment. Typical system transfer functions, prior to gain amplification by the recorder, are shown in Figures 3 and 4

---

1. Dean, J.S. (1969) Chronological Analysis of Tsegi Phase Sites in Northeastern Arizona. *Papers of the Laboratory of Tree-Ring Research*, No. 3, University of Arizona Press.

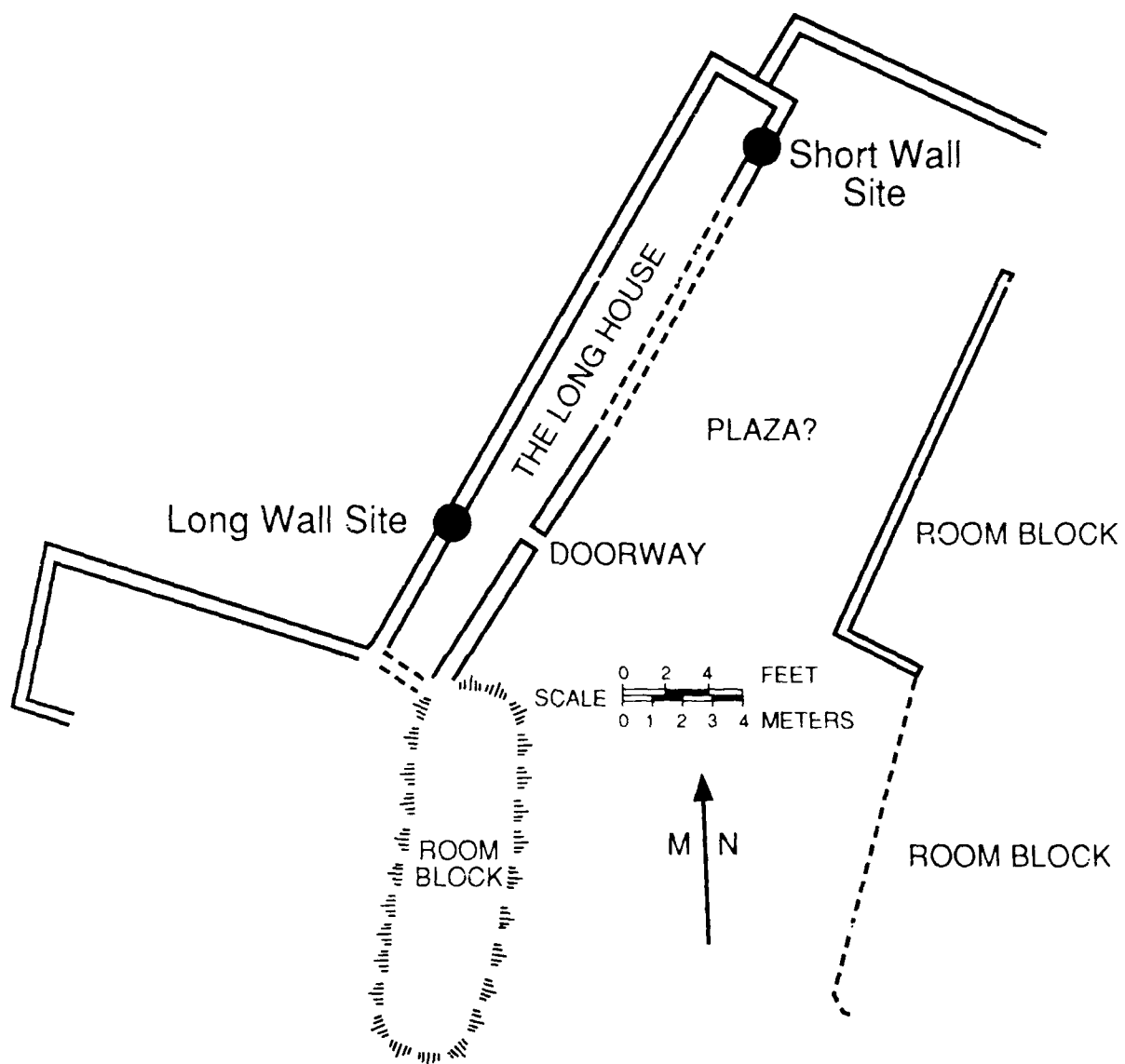


Figure 2. Plan View of Long House Ruins Showing the Instrument Locations

Table 1. Instrument Constants for Pressure and Seismic Transducers

Site	Location	Recorder S/N	Sensor S/N	Sensitivity (V/(m/sec))	Constants	
					F <sub>0</sub> (Hz)	B <sub>0</sub>
1	Bottom Long Wall	320	9324	100.706	1.96	0.429
				91.216	2.05	0.380
				102.567	2.38	0.348
2	Top Long Wall	334	9319	100.805	2.04	0.422
				115.826	1.98	0.432
				100.351	2.43	0.355
3	Pressures Long Wall		PT-1	0.000735 V/Pa		
			PT-2	0.000713 V/Pa		
			PT-3	0.000724 V/Pa		
4	Bottom Short Wall	281	9261	113.396	1.99	0.452
				115.261	2.07	0.410
				109.998	2.60	0.348
5	Top Short Wall	278	9325	112.377	2.03	0.417
				105.186	2.06	0.433
				102.130	2.38	0.349
6	Pressures Short Wall	280	PT-5	0.000723 V/Pa		
			PT-7	0.000721 V/Pa		
			PT-9	0.000723 V/Pa		

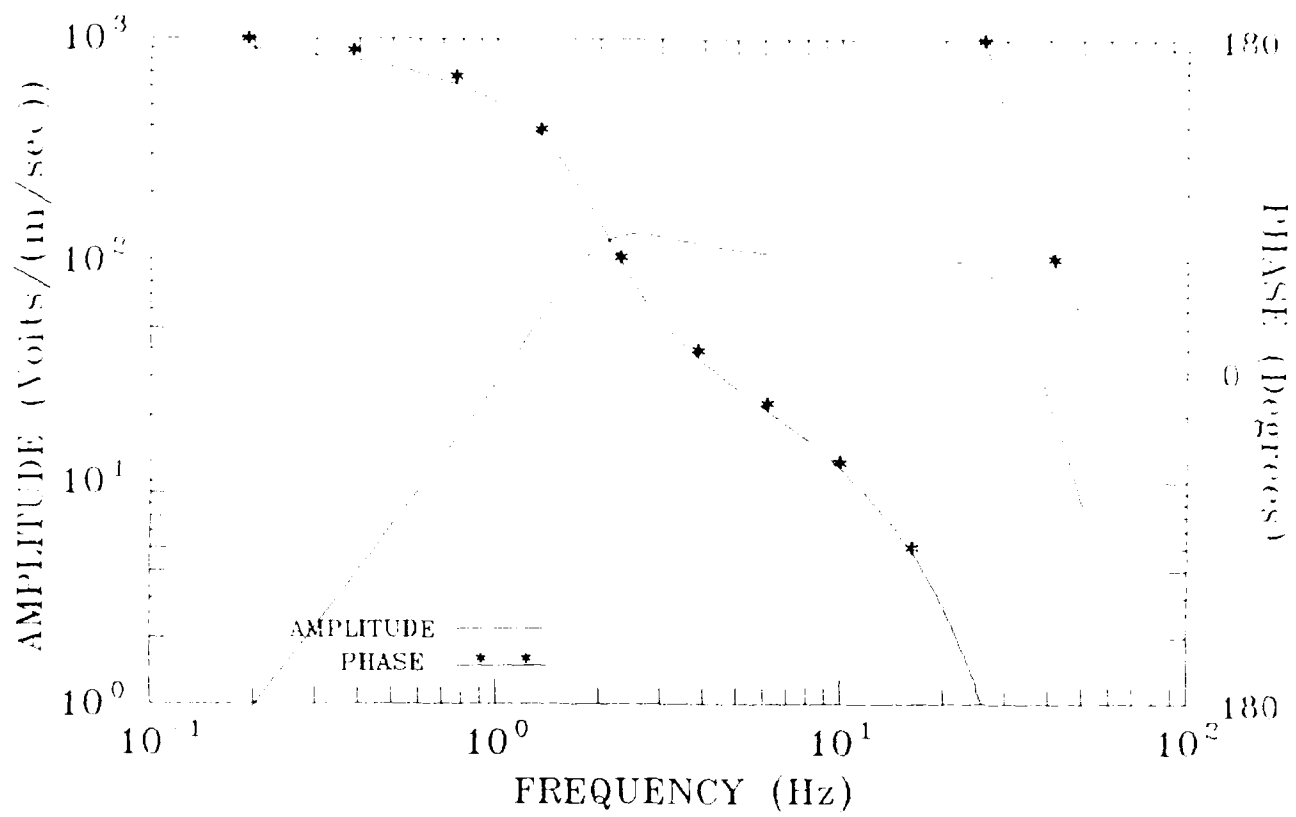


Figure 3. Typical Instrument Response Function for a Dyneer S-6000 Seismometer Recorded Through a DCS-302 Field Recorder

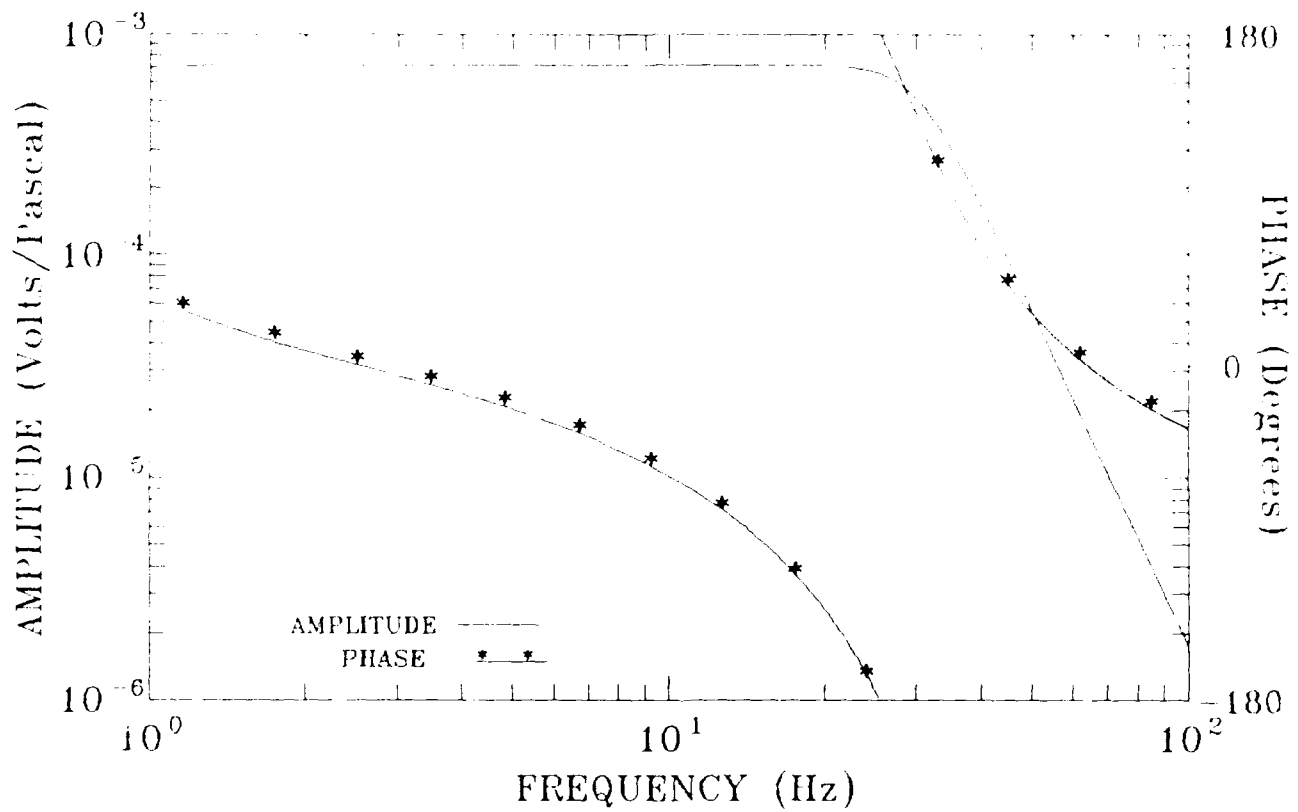


Figure 4. Typical Instrument Response Function for a DJ Instruments Differential Pressure Transducer Recorded Through a DCS-302 Field Recorder

for a seismometer and pressure transducer, respectively. A reliable estimate of pressure and ground velocity can be achieved in a band of at least 1.0 to 30 Hz for the 100 sample per second recorders and 1.0 to 70 Hz for the 200 sample per second data.

#### **4. VIBRATION CRITERIA**

Evaluation of the effects of overflights on archaeological structures requires some criteria with which to compare the induced vibrations. Previous investigators have used values at or above 1.3 mm/sec ( $1.3 \times 10^{-3}$  m/sec) as safe maximum allowable levels for ancient structures.<sup>2,3</sup> In particular, King, Algermissen and McDermott applied a criterion of 2.0 mm/sec over a bandwidth of 1 to 20 Hz during studies on structures similar to the Long House site. For this study, vector sum velocities below 1.3 mm/sec in the bandwidth of 1 to 40 Hz are considered to be safe for ancient structures. Both the lower amplitude and wider bandwidth of this criterion as compared to that used in the Chaco Canyon study should ensure that the criterion represents a conservative threshold.

#### **5. AIRCRAFT OVERFLIGHTS**

Aircraft overflights by a B-52, an RF-4C and two A-7 aircraft were monitored at the Long House sites. For most overflights, the aircrews reported heading, altitude, and indicated and true air speed. In addition, a ground observer at the site estimated the horizontal range at closest approach to the site. During the B-52 overflights, good quality pressure measurements were obtained. For the RF-4C and A-7 overflights the pressure data were unusable due to recorder malfunctions.

During the occupation of the Long House site, more than 37 overflights were monitored. These were distributed as 16 B-52 overflights, 5 passes by the RF-4C and at least 16 passes by the A-7s. The number of distinct overflights for the A-7 is not well defined as the two aircraft would sometimes overfly the site with very short time separations. Lacking pressure time histories, it is not always possible to separate the motions induced by one overflight from those of a subsequent pass. Aircraft data on the identified passes for each type of aircraft are given in Tables 2 through 4.

##### **5.1 B-52 Pressure Signatures**

Pressure signatures recorded for the B-52 overflights at Long House define a general pattern that should be consistent for any low and close overflight by other types of aircraft. Basically, the pressure signature of an overflight can be broken into three elements, the distant approach, near closest approach, and departure. These elements are demonstrated in Figure 5, the time histories from three

- 
2. King, W.K., Algermissen, S.T., and McDermott, P.J. (1985) *Seismic and Vibration Hazard Investigation of Chaco Culture National Historic Park*, Open File Report 85-529, U.S. Geological Survey, Denver, CO.
  3. Saurenman, H.J., Nelson, J.T., and Wilson, G.P. (1982) *Handbook of Urban Rail Noise and Vibration Control*, DOT Report No. DOT-TSC-UMTA-81-72, Wilson, Ihrig & Associates, Oakland, CA.

Table 2. B-52 Overflight Data

Over-Flight	Time	Heading	Altitude (m AGL)	Air Speed (m/sec)		Range* (m)	Max. Sound Pressure (dB) <sup>1</sup>
				Indicated	True		
0	1423	N-S*	>300*	-	-		98.4
1	1427	S-N*	300*	-	-	300W	97.0
2	1431	N-S*	150	134	159	300E	96.2
3	1435	N-S*	180	139	159	150W	98.7
4	1443	070	150	157	180	300N	104.8
5	1448	275	180	141	170	30W	99.8
6	1453	100	190	144	170	0	106.9
7	1458	010	180	149	175	600N	98.0
8	1503	225	120	144	170	300N	98.3
9	1510	048	150	139	165	0	102.6
10	1516	225	150	149	175	600S	94.9
11	1522	030	210	134	159	600S	99.0
12	1530	264	210	149	175	0	104.5
13	1536	078	180	154	180	60E	113.3
14	1541	310	210	149	175	0	101.0
15	1548	160	210	144	170	30W	104.1

\*NOTE: Values estimated by observer

<sup>1</sup>Re  $2 \times 10^{-5}$  Pa

Table 3. RF-4C Overflight Data

Over-Flight	Time	Heading	Altitude (m AGL)	Air Speed (m/sec)		Max. Sound Pressure (dB) <sup>1</sup>
				Indicated	True	
1	1015	360	300	246	273	-
2	1018	090	150	246	273	-
3	1020	090	150	246	273	-
4	1022	090	150	246	273	-
5	1025	090	150	246	273	-

\*NOTE: Air speed confirmed only after first pass.

<sup>1</sup>Unavailable due to equipment malfunction.

Table 4. A-7 Overflight Data

Over-Flight	Time	Heading	Altitude (m AGL)	Ground Speed (m/sec)	Max. Sound Pressure (dB) <sup>1</sup>
0	1403.2	260	90	231	-
1	1404.2	265	120	236	-
2	1405.1	265	120	226	-
3	1405.5	270	90	221	-
4	1406.5	300	120	231	-
5	1407.2	300	120	226	-
6	1408.1	300	90	226	-
7	1408.3	360	60	226	-
8	1409.0	360	90	226	-
9	1409.4	015	60	247	-
10	1410.2	015	90	226	-
11	1411.2	015	60	236	-
12	1411.5	060	60	226	-
13	1412.2	057	60	241	-
14	1413.0	090	90	226	-
15	1413.8	090	60	247	-

<sup>1</sup>Unavailable due to equipment malfunction.



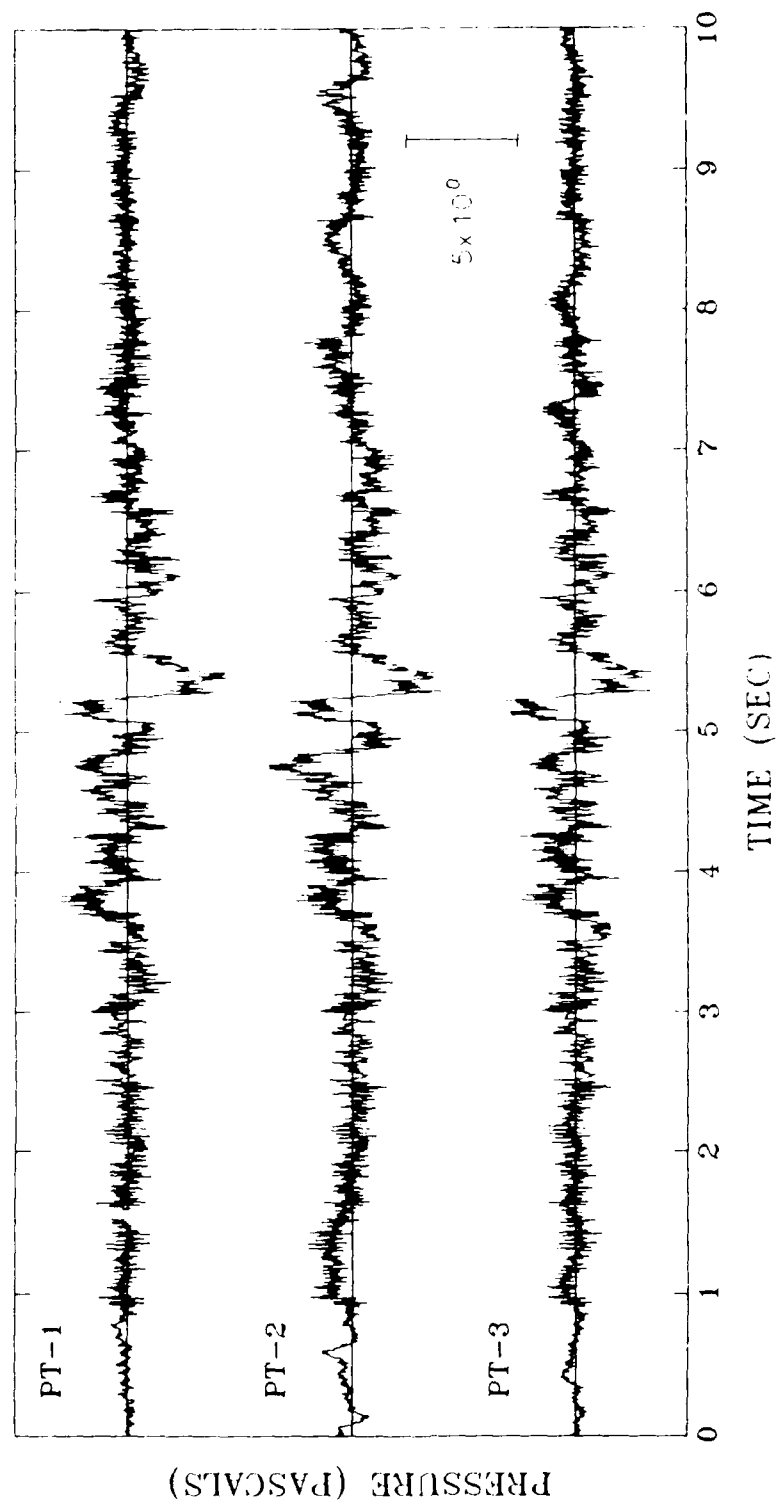


Figure 5. Typical Pressure Time History of a B-52 Overflight as Recorded at the Long House Site (Pass 6)

essentially collocated transducers during B-52 pass 6. Wind conditions during the B-52 overflights were considered light to near calm. A pressure noise spectrum for the B-52 overflights is shown in Figure 6 and demonstrates the classical roll-off of wind noise with frequency.<sup>4</sup> This spectral estimate is based on data taken at the beginning of overflight 6 with the B-52 at a range of approximately 6000 meters.

On approach to the Long House, the pressure signals of the B-52 emerge out of the pressure noise approximately 5 to 7 seconds prior to the time of closest approach and continue to grow in strength. Given the air speed for the overflights, the initial time of detection is equivalent to a range of about 1000 meters. In Figure 5 the time history for overflight 6, the onset of the B-52 signature is readily apparent near the 1-second mark of the plot. Figure 7 is the power spectral density estimate of the signature just after detection. Comparison with Figure 6 shows a definite increase in energy above 30 Hz but no significant change below that frequency. On approach the dominant aero-acoustics are likely to be engine compressor and air frame noise.<sup>5</sup>

At the 5-second mark in Figure 5, a pronounced low frequency pulse overrides the engine and airframe noise and is correlated with the close approach of the aircraft to the observation point. Measurements taken during this experiment were insufficient to define the exact nature of this pulse. It is not inconsistent, however, with the dynamic pressure of the turbulent wake of the aircraft.<sup>6,7</sup> This pulse is seen in Figure 8, the pressure spectral estimate for the aircraft overhead, as a broad increase in energy over the window from about 2 to 70 Hz.

For the departing aircraft a persistent, higher frequency signal was recorded and can be associated with engine jet noise.<sup>5</sup> The spectral content of the signal at 5 seconds out from the site is seen in Figure 9. On comparison with Figures 7 and 8, it is apparent that a greater proportion of the energy was in the range above 30 Hz although there remained a significant peak in the area of 30 Hz. The signals recorded during departure tended to be modulated and were apparent for many tens of seconds after the aircraft passed overhead. In some cases, appreciable signal strength was detected 50 seconds or more after the B-52 had passed.

The peak pressures measured at Long House were associated with the low frequency pulse occurring at or very near to the time of closest approach of the B-52s. The observed pressures, given in terms of dB, relative to  $2 \times 10^{-5}$  Pa, are listed in Table 2. These pressures can be interpreted in terms of an equivalent wind velocity through the relationship:

- 
4. Bruce, R.D. (1971) *Field Measurements: Equipment and Techniques, Noise and Vibration Control*, L.L. Beranek, Ed., McGraw-Hill Book Co., New York.
  5. Grieb, H., and Heinig, K. (1986) *Noise Emission of Civil and Military Aero-Engines - Sources of Generation and Measures of Attenuation, Aircraft Noise in a Modern Society*, H.J. Gummlich and H.D. Marohn, NATO Committee on the Challenges of Modern Society Report No. 161, Mittenwald, Germany.
  6. Bisgood, P.L., Maltby, R.L., and Dee, F.W. (1971) *Some work at the Royal Aircraft Establishment on the behavior of vortex wakes, Aircraft Wake Turbulence and Its Detection*, J.H. Olsen, A. Goldberg, and M. Rogers, Eds., Plenum Press, New York.
  7. Garodz, L.J., Lawrence, D.M., and Miller, N.J. (1976) *Measurement of the Trailing Vortex Systems of Large Transport Aircraft Using Tower Fly-By and Flow Visualization (Summary, Comparison, and Application)*, FAA-RD-75-127, ADA 021305, Atlantic City, N.J.

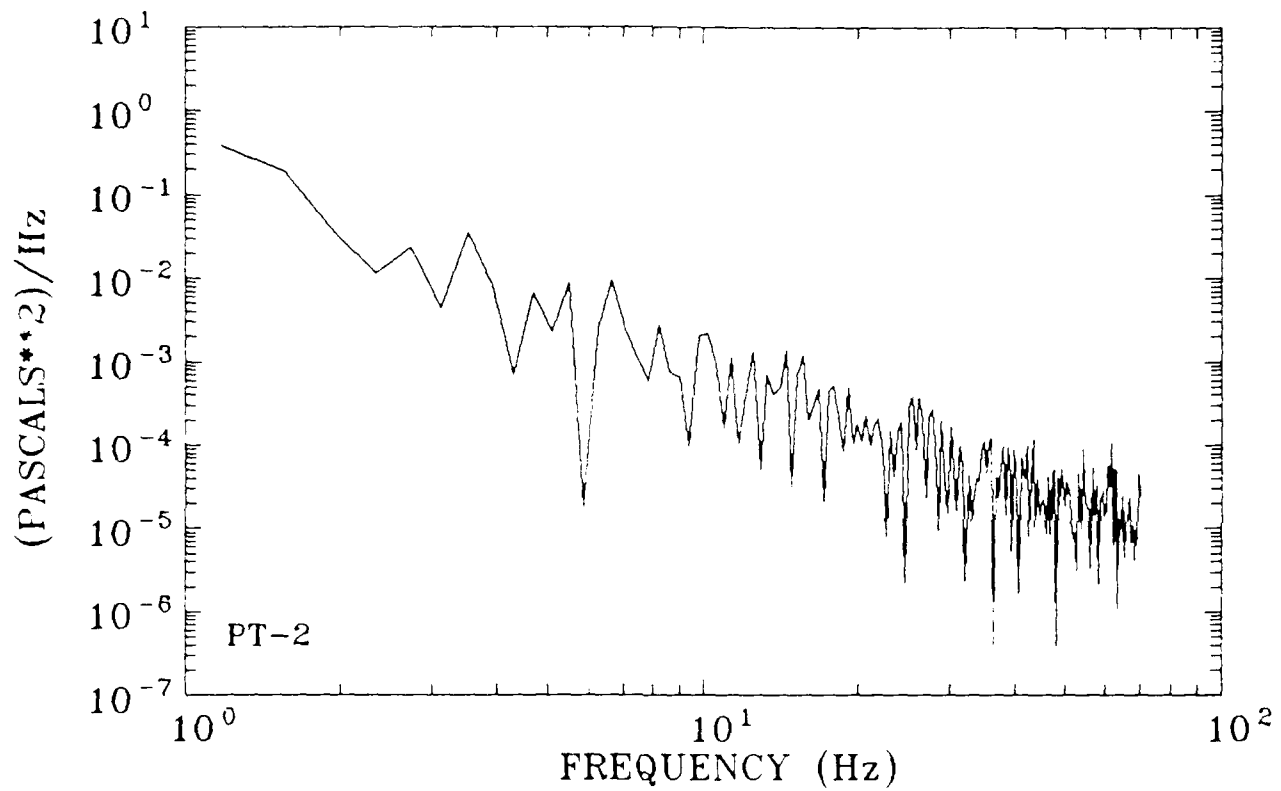


Figure 6. Spectral Estimate of the Pressure Background Noise Just Prior to B-52 Pass 6. (Aircraft at a range of 6000 meters)

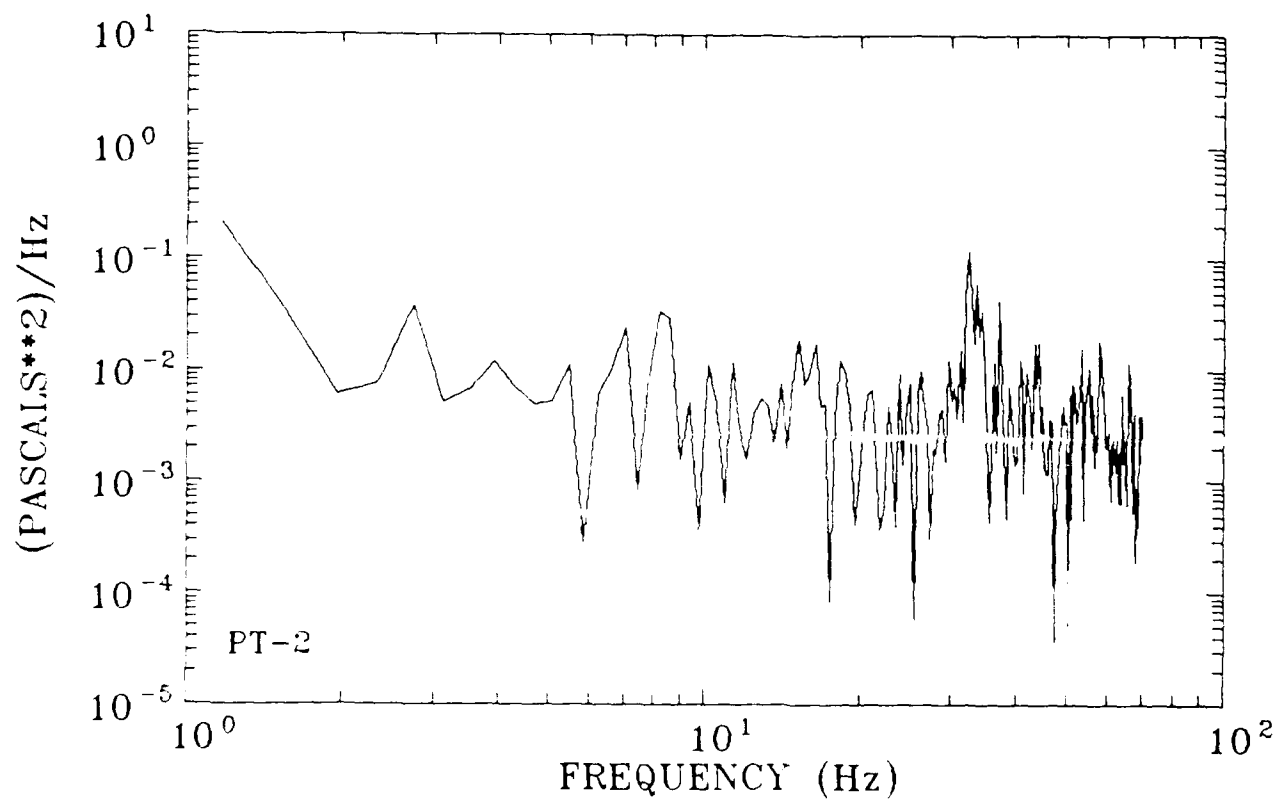


Figure 7. Spectral Estimate of the Pressure Signal for B-52 Overflight 6 on Approach to Long House (Aircraft at a range of 6000 meters)

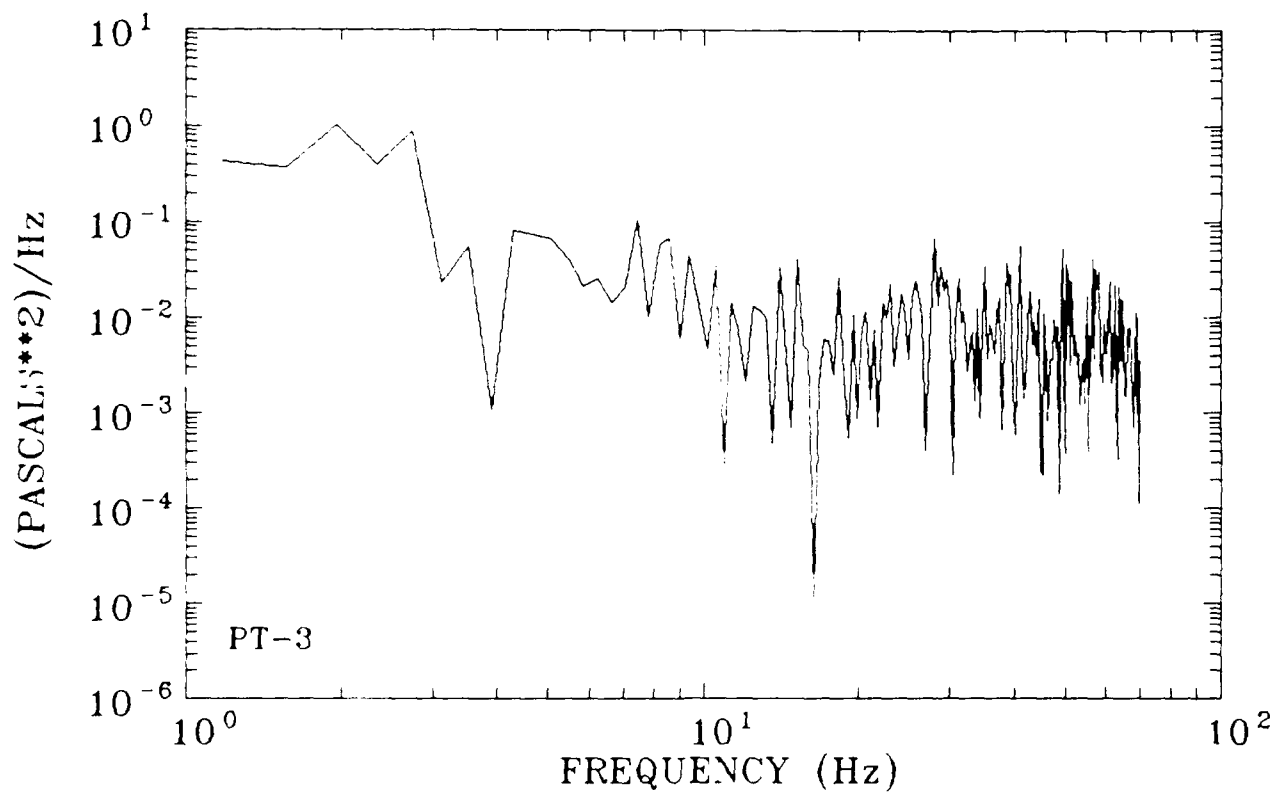


Figure 8. Spectral Estimate of the Pressure Signal for B-52 Overflight 6 Overhead

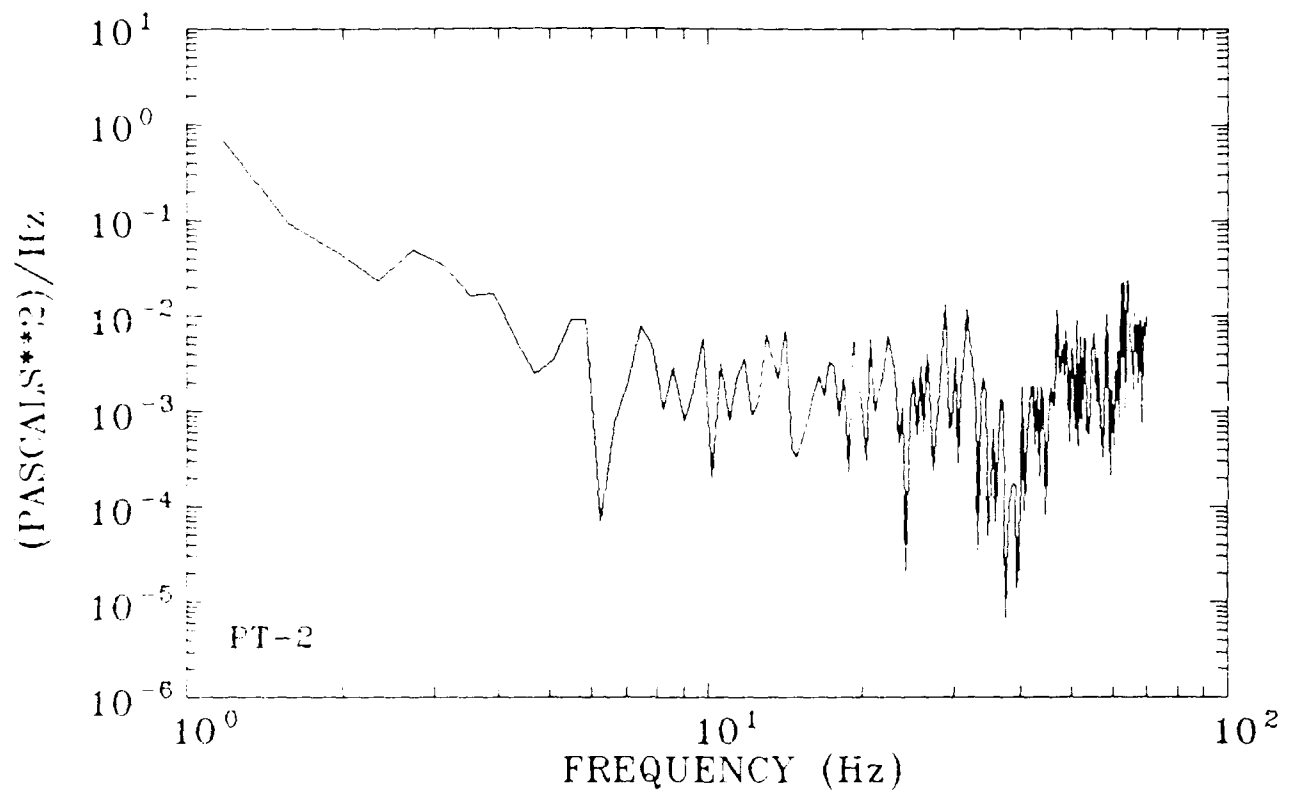


Figure 9. Spectral Estimate of the Pressure Signal for B-52 Overflight 6 Departing from the Long House Sites (Aircraft at a Range of 600 meters)

$$V = ((2q)/\rho)^{1/2} \quad (1)$$

where  $q$  is the measured pressure,  $\rho$  is the unit density of air and  $V$  is the equivalent wind velocity.<sup>8</sup> Using a standard value for  $\rho$  of 1.23 kg/m<sup>3</sup>, the maximum observed pressure for all B-52 overflights, less than 10 Pa, is found to be equivalent to a wind gust of less than 4.0 m/sec.<sup>9</sup>

## 5.2 RF-4C and A-7 Pressure Signals

Although pressure data were not recorded for the overflights of the RF-4C and A-7 aircraft, some discussion of the probable signals relative to those of the B-52 is warranted. The general pressure signal pattern during overflights, as described above for the B-52, should also hold for the smaller airplanes. Due to relative sizes of the aircraft and the higher jet exhaust velocities typically associated with engines of the smaller planes, it should be anticipated that the spectral content of the airframe and engine acoustics would be at higher frequencies than those of the B-52. In addition, as these airplanes overflew the site at lower altitudes and with higher velocities, it should be expected that these planes would produce broadband higher amplitude signals at the ground and thus higher loads on the Long House structure than the B-52 overflights.

During both the RF-4C and A-7 overflights, significantly higher wind velocities were noted at Long House than during the B-52 overflights. No attempt was made to estimate the wind speeds however.

## 6. LONG HOUSE OVERFLIGHT RESPONSES

Vibration was measured at the two Long House sites during all aircraft overflights including the RF-4C and A-7 passes for which no pressure data were obtained. Maximum particle velocities recorded at the top of each wall segment during each overflight are given in Tables 5 through 7. As has been anticipated, the peak motions were recorded on the components normal to the axes of the walls while the vertical particle velocities are well below the horizontal levels.

Foundation level amplitudes, sites 1 and 4, were typically an order of magnitude or more below those at the top of the wall. These motions also echoed the frequency content of the upper wall data. This spectral similarity leads to two desirable conclusions. First, the foundation signal is dominated by the resonant frequencies of the wall, which implies that the overflight vibrations are induced by the direct pressure loading on the wall with little or no energy transmission into the structure from the ground. Further, the spectral similarity at the top and bottom of the walls demonstrates that the observed motions are the motions of the wall as a unit and not significantly modified by poor coupling of the seismometers to the walls or other localized conditions.

---

8. Houghton, E.L., and Carruthers, N.B. (1976) *Wind Forces on Buildings and Structures: An Introduction*, John Wiley & Sons, New York.

9. Champion, K.S.W., Cole, A.E., and Kantor, A.J. (1985) *Standard and Reference Atmospheres, Handbook of Geophysics and the Space Environment*, A.S. Jurse, Ed., Air Force Geophysics Laboratory, AFGL-TR-85-0315, ADA 167000, Hanscom AFB, MA.

Table 5. Maximum Wall Velocities at Long House for B-52 Overflights

Over- Flight	Comp	Site 2 Long Wall ( $10^{-5}$ m/sec)	Site 5 Short Wall ( $10^{-5}$ m/sec)
0	N42E	1.92	6.42*
	N48W	4.32	8.66*
	VERT	0.32	1.10*
	VECTOR SUM	4.73	10.84
1	N42E	1.84	3.56
	N48W	4.14	6.08
	VERT	0.26	0.54
	VECTOR SUM	7.10	7.06
2	N42E	2.24	2.80
	N48W	4.98	6.48
	VERT	0.44	0.90
	VECTOR SUM	5.48	7.12
3	N42E	2.40	2.88
	N48W	5.40	7.54
	VERT	0.41	0.90
	VECTOR SUM	5.92	8.12
4	N42E	4.50	5.98
	N48W	7.00	5.72
	VERT	1.18	0.86
	VECTOR SUM	7.38	4.13
5	N42E	2.82	3.36
	N48W	9.50	6.22
	VERT	0.72	0.98
	VECTOR SUM	9.94	7.14
6	N42E	4.26	3.36
	N48W	6.38	6.22
	VERT	0.80	1.50
	VECTOR SUM	8.56	7.22
7	N42E	3.44	-
	N48W	4.10	-
	VERT	0.34	-
	VECTOR SUM	5.36	-



Table 5. Maximum Wall Velocities at Long House for B-52 Overflights (Cont.)

Over-Flight	Comp	Site 2 Long Wall ( $10^{-5}$ m/sec)	Site 5 Short Wall ( $10^{-5}$ m/sec)
8	N42E	2.56	4.36
	N48W	4.20	6.56
	VERT	0.32	0.70
	VECTOR SUM	4.92	7.90
9	N42E	2.06	4.16
	N48W	4.00	11.54
	VERT	0.38	1.64
	VECTOR SUM	4.52	12.38
11	N42E	2.24	10.06
	N48W	2.86	12.60
	VERT	0.26	0.96
	VECTOR SUM	3.84	16.16
12	N42E	3.42	4.82
	N48W	15.54	10.22
	VERT	1.08	1.12
	VECTOR SUM	15.90	11.36
13	N42E	3.60	12.84
	N48W	11.92	20.10
	VERT	0.96	2.38
	VECTOR SUM	12.44	23.96
14	N42E	4.70	12.16*
	N48W	21.48	9.90
	VERT	1.92	1.66*
	VECTOR SUM	22.16	15.76
15	N42E	3.14	3.54
	N48W	9.44	7.22
	VERT	0.62	1.06
	VECTOR SUM	9.94	8.12

NOTE. Maximum vibrations appear to result from extraneous ground input, not pressure loading.

Table 6. Maximum Wall Velocities at Long House for RF-4C Overflights

Over- Flight	Comp	Site 2 Long Wall ( $10^{-5}$ m/sec)	Site 5 Short Wall ( $10^{-5}$ m/sec)
0	N42E	0.52	0.68
	N48W	0.74	1.06
	VERT	0.08	0.14
	VECTOR SUM	0.90	1.26
1	N42E	0.74	0.80
	N48W	1.26	2.10
	VERT	0.14	0.38
	VECTOR SUM	1.46	2.28
2	N42E	7.88	10.78
	N48W	21.42	22.34
	VERT	1.74	3.12
	VECTOR SUM	22.86	25.00
3	N42E	7.52	13.94
	N48W	38.50	29.14
	VERT	2.90	3.16
	VECTOR SUM	39.76	32.04
4	N42E	7.59	10.44
	N48W	18.88	31.44
	VERT	1.46	3.74
	VECTOR SUM	20.40	33.34
5	N42E	12.46	17.86
	N48W	31.66	46.42
	VERT	3.58	6.12
	VECTOR SUM	34.22	50.12

Table 7. Maximum Wall Velocities at Long House for A-7 Overflights

Over- Flight	Comp	Site 2 Long Wall ( $10^{-5}$ m/sec)	Site 5 Short Wall ( $10^{-5}$ m/sec)
0	N42E	6.02	10.12
	N48W	9.86	14.02
	VERT	0.80	1.44
	VECTOR SUM	11.58	17.36
1	N42E	4.74	11.86
	N48W	7.70	17.28
	VERT	0.64	2.26
	VECTOR SUM	9.06	21.08
2	N42E	3.66	3.52
	N48W	12.32	15.02
	VERT	1.10	2.10
	VECTOR SUM	13.60	16.14
3	N42E	10.78	7.12
	N48W	17.96	16.98
	VERT	1.42	2.44
	VECTOR SUM	21.00	18.58
4	N42E	7.18	4.96
	N48W	15.30	13.00
	VERT	0.96	1.84
	VECTOR SUM	16.92	14.04
5	N42E	6.16	4.74
	N48W	20.68	9.64
	VERT	1.36	1.20
	VECTOR SUM	21.62	10.80
6	N42E	4.30	6.36
	N48W	4.88	9.34
	VERT	0.54	1.18
	VECTOR SUM	6.52	11.36
7	N42E	4.12	4.46
	N48W	9.08	6.82
	VERT	0.70	0.70
	VECTOR SUM	10.00	8.18

## 6.1 B-52 Overflight Responses

Time traces of the upper wall responses for B-52 pass 6 are shown in Figures 10 and 11. These traces show the response of the two wall segments during the identical time window as that used for the pressure data in Figure 5. A cursory inspection of these two figures clearly demonstrates the importance of the unique characteristics of the walls in defining the motion response. Most notably one can see the effect of the maximum pressure pulse from the aircraft 5 seconds into the record on the response of site 5 and the lack of reaction to the same event at site 2.

In this case, and for virtually all other B-52 overflights, the peak velocities at either site did not correlate with the occurrence of the peak pressure pulse from the aircraft. (Note that the vibrations at site 5 during overflight 6 induced by the peak pressure pulse are not the maximum velocities recorded at this site during this pass. The maximum motions are completely outside the displayed window.) Separations of 10 seconds or more between the peak pressure signal and the maximum wall responses are typical with the wall response leading the pressures on some occasions and trailing on others. No discernible relationship between the separation times and aircraft heading has been noted.

As is obvious from the very narrow band responses at both sites, the wall vibrations result from the coupling of the airframe or engine acoustics with the higher resonant modes of the walls. This is further emphasized by the definite resonant peaks seen in the maximum entropy spectral estimates of wall motions as shown in Figure 12 and 13. For site 2, the long wall segment, a relatively simple structure is seen in the excitation functions. Normal to the axis of the wall resonance occurs at approximately 6.5 and 25.0 Hz while along the wall axis it occurs at 29.0 Hz. A more complex response is seen at site 5 with modes at 6.5, 14.5, 21.0, and 25.0 Hz normal to the axis of the wall and 29.0 and 38.0 Hz along the axis. Due to the less regular shape of the short wall segment and the more eroded mortar bonds in this wall, the complex response function is not unexpected. The location of these modes are comparable to those found by King, Algermissen, and McDermott for similar sites at Chaco Canyon.<sup>2</sup>

A rudimentary correlation analysis of the vibration data with parameters of the aircraft approach, such as heading, air speed, altitude, and range, indicate little sensitivity of the wall response to any factor other than aircraft range.

During all B-52 overflights, both the short and long wall responses were over a factor of 5 below the maximum safe vibration level of 1.3 mm/sec. Given that this criterion most likely represents a conservative limit and that the level was not approached during the overflights, it is concluded that B-52 overflights at altitudes above 150 meters AGL do not constitute a significant threat to archaeological structures similar to Long House.

## 6.2 RF-4C and A-7 Overflight Responses

Wall responses were also recorded for RF-4C and A-7 overflights. Figure 14 through 17 show the maximum response of each wall segment to passes by both aircraft types. Overflights by these aircraft were performed at generally higher ground speeds and lower altitudes than for the B-52s. As expected, they produced larger responses in both wall segments. The recorded wall motions were larger, in the worst cases, by a factor of about 2 than those observed during B-52 overflights. Responses remained nearly a factor of 2 below the vibration criterion for ancient structures.

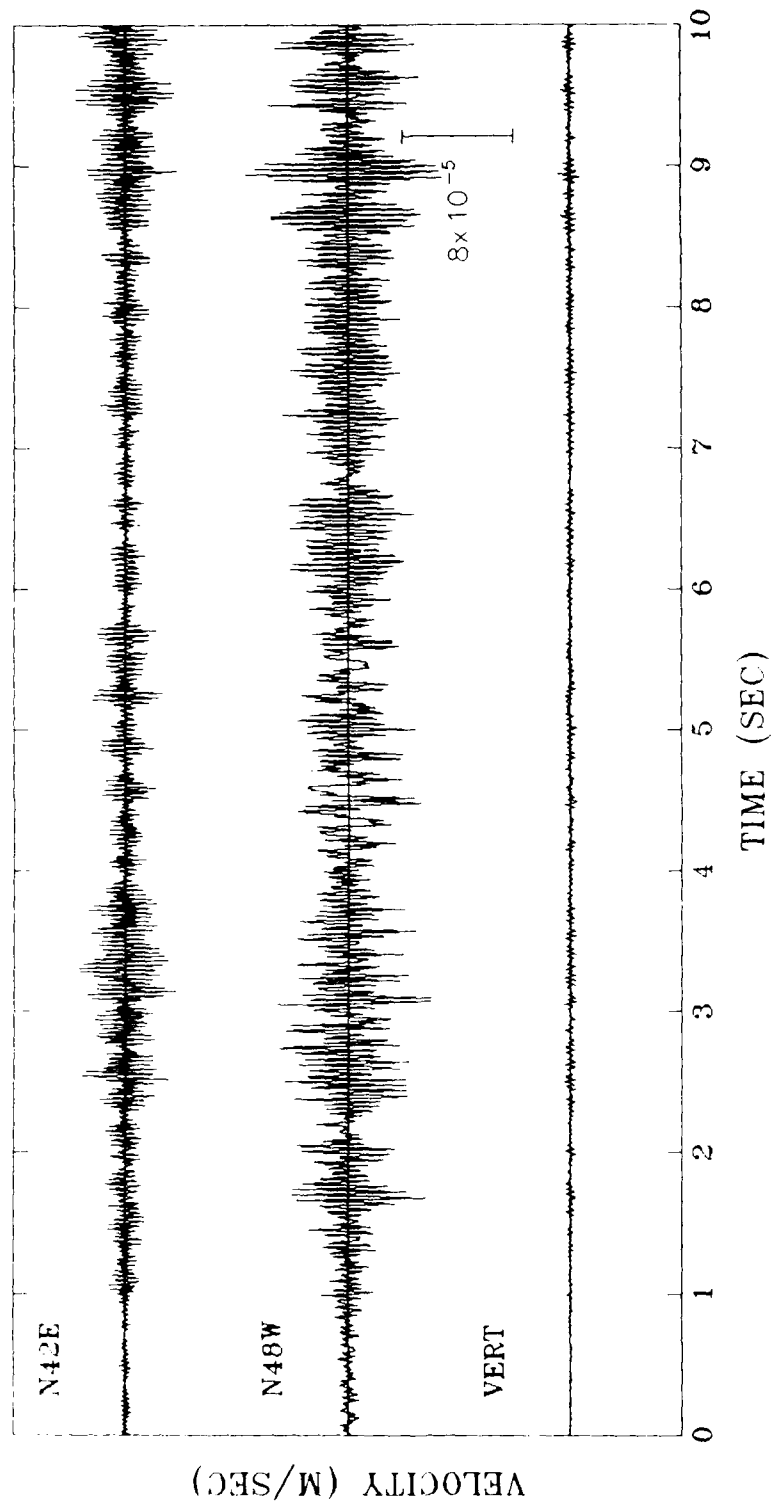


Figure 10. Long Wall Segment Response for B-52 Overflight 6

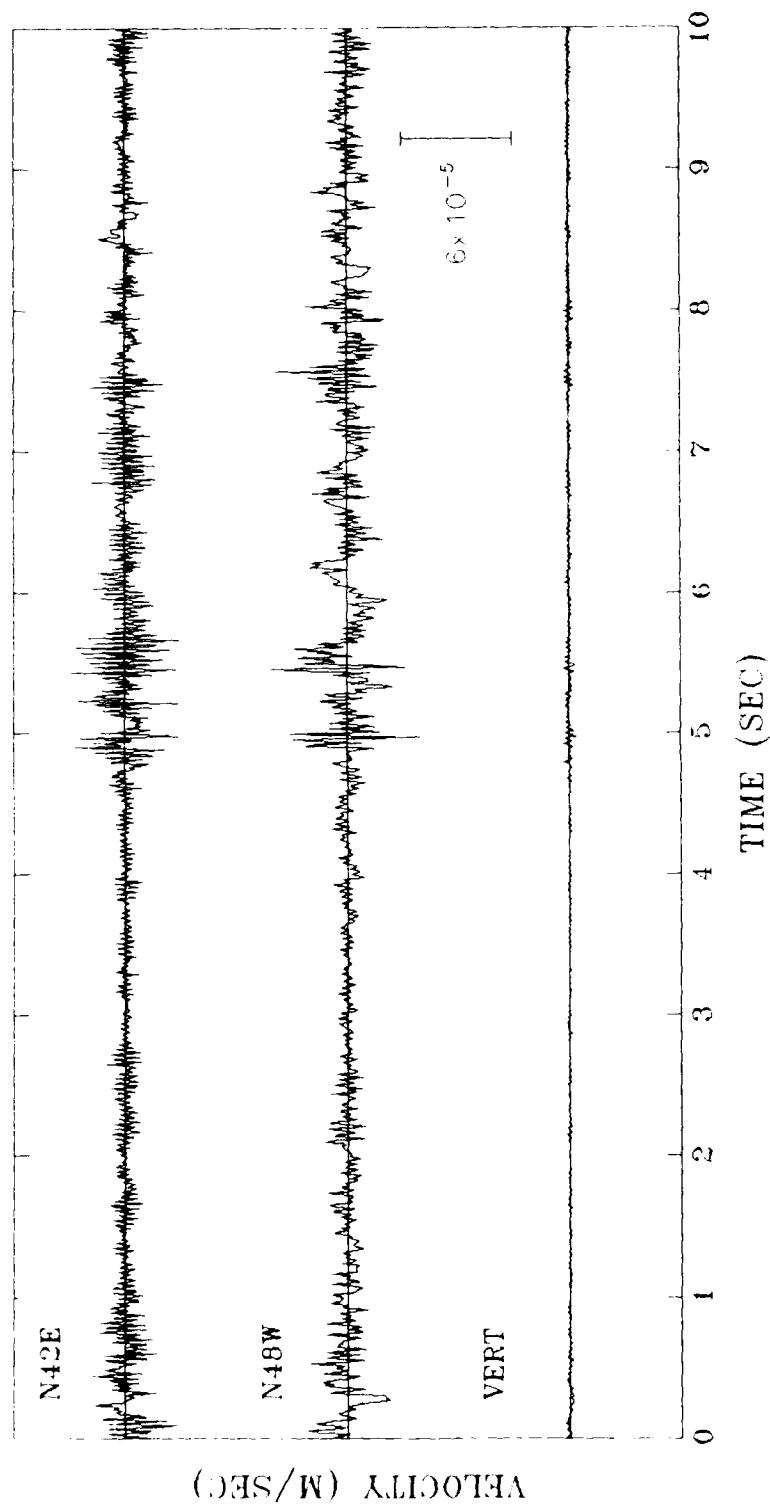


Figure 11. Short Wall Segment Response for B-52 Overflight 6

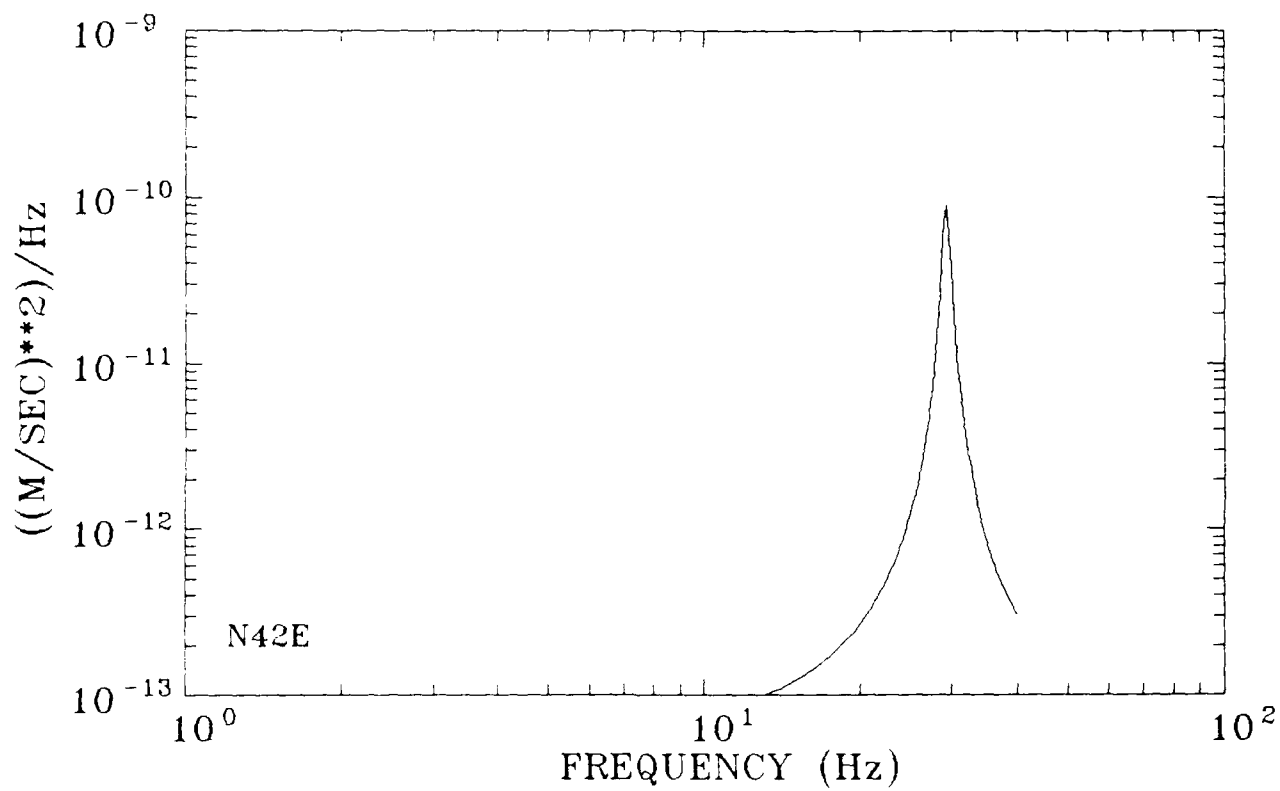


Figure 12a. Maximum Entropy Spectral Estimates of the Wall Motions at Site 2, the Long Wall Segment, During B-52 Overflight 6. Components of motion are N42E.

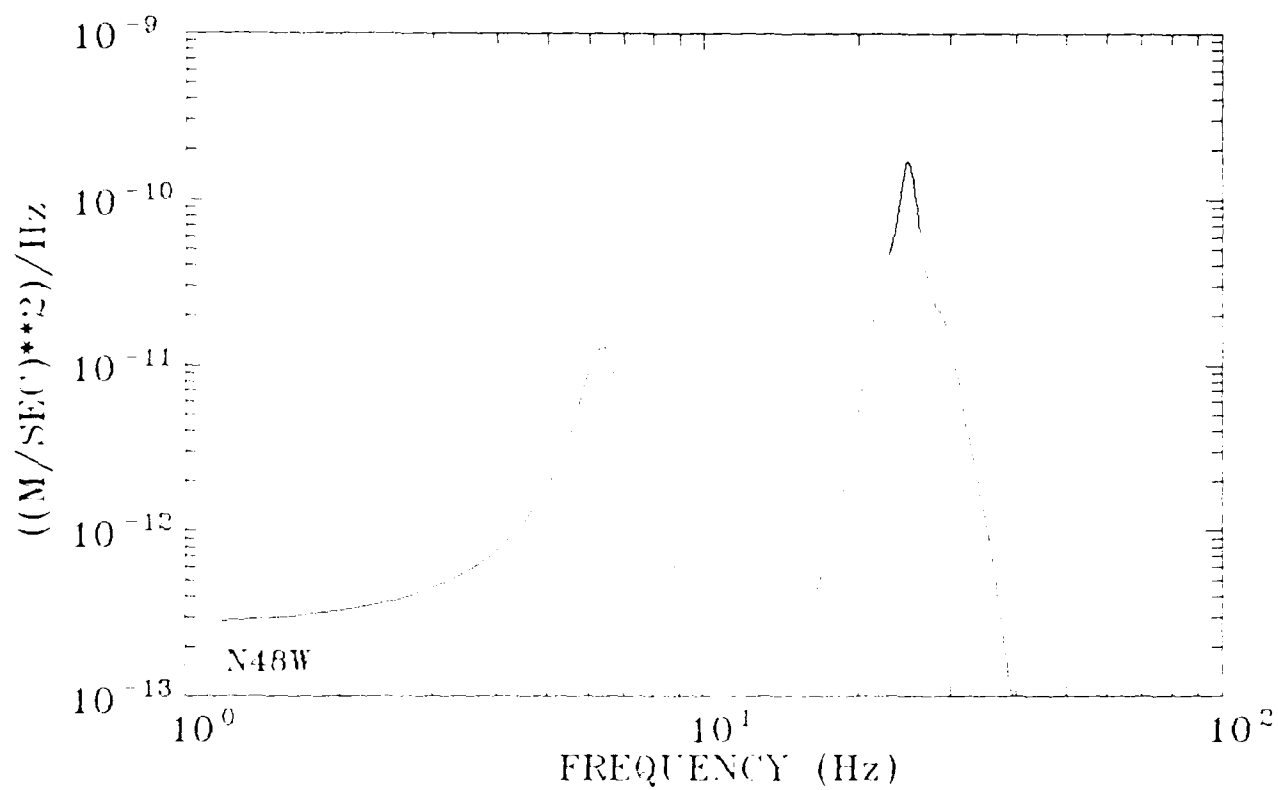


Figure 12b. Maximum Entropy Spectral Estimates of the Wall Motions at Site 2, the Long Wall Segment, During B-52 Overflight 6. Components of motion are N48W.



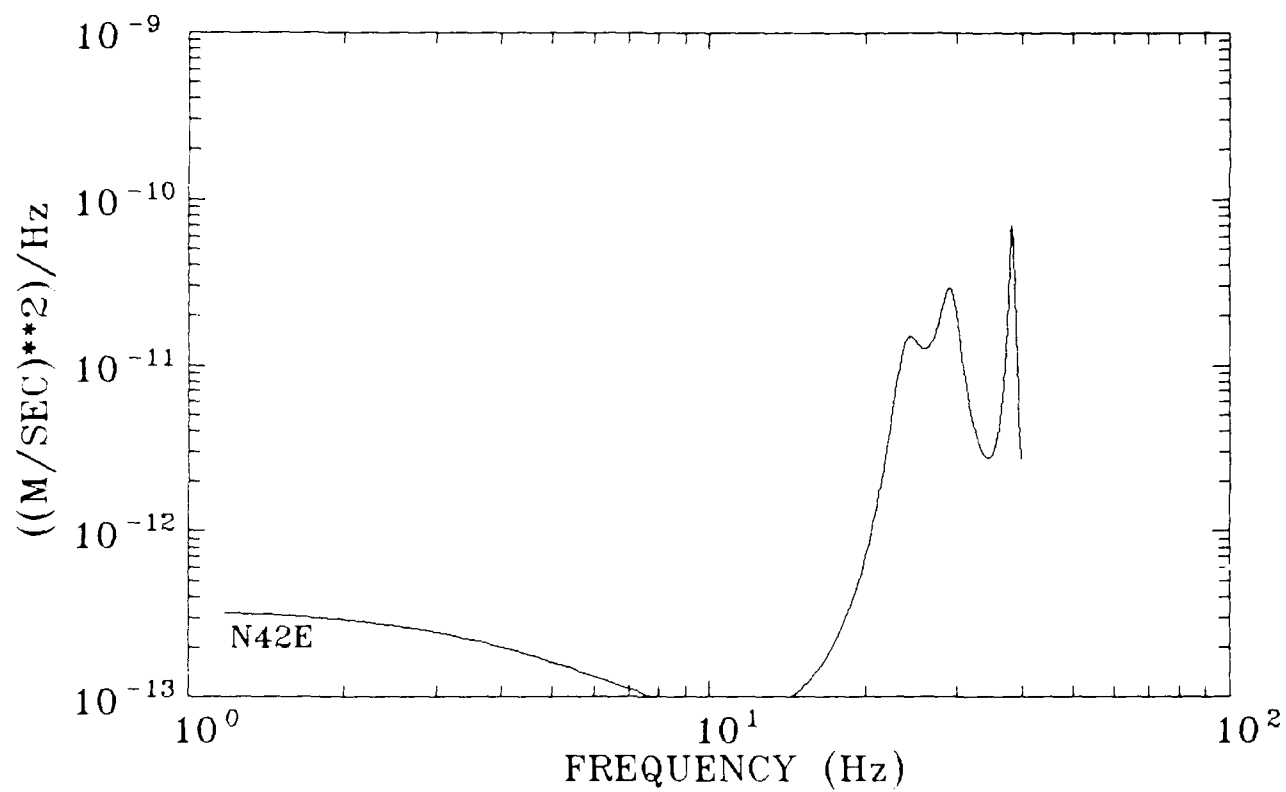


Figure 13a. Maximum Entropy Spectral Estimates of the Wall Motions at Site 5, the Long Wall Segment, During B-52 Overflight 6. Components of motion are N42E.

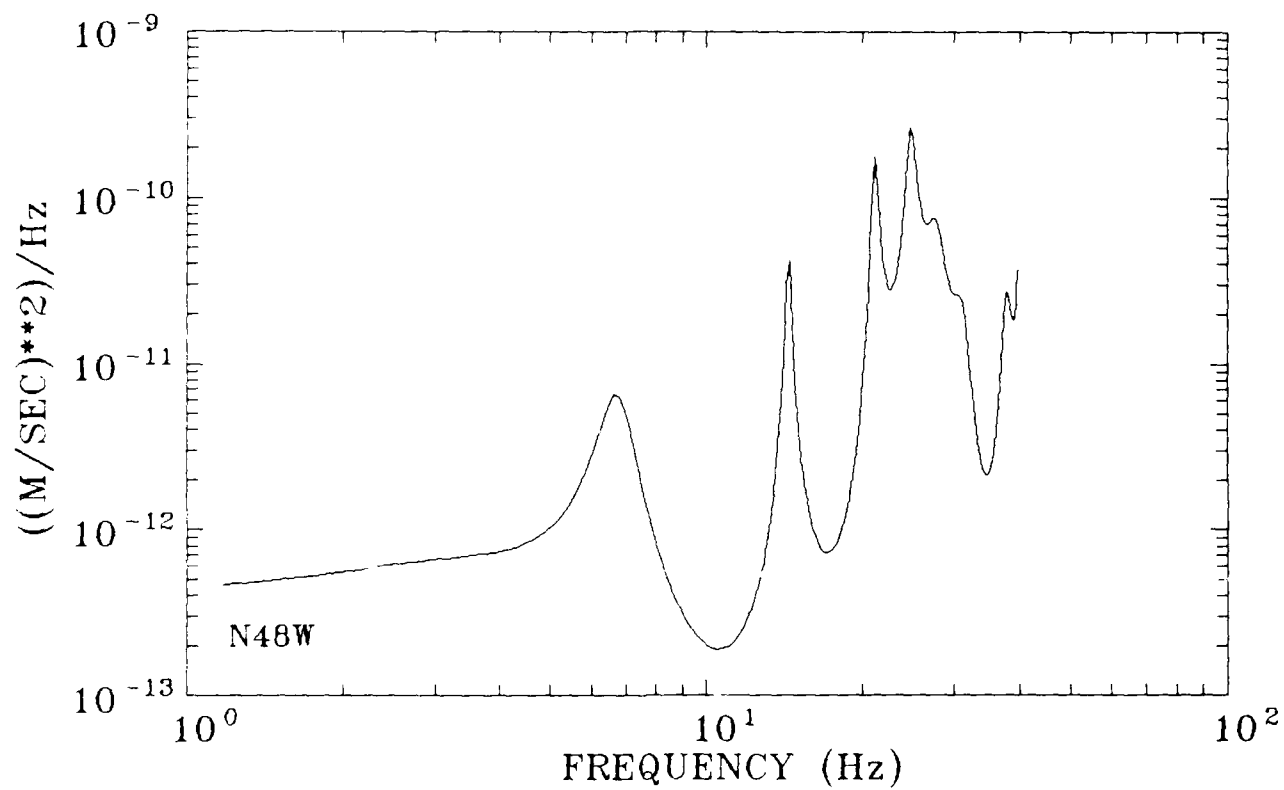


Figure 13b. Maximum Entropy Spectral Estimates of the Wall Motions at Site 5, the Long Wall Segment, During B-52 Overflight 6. Components of motion are N48W.

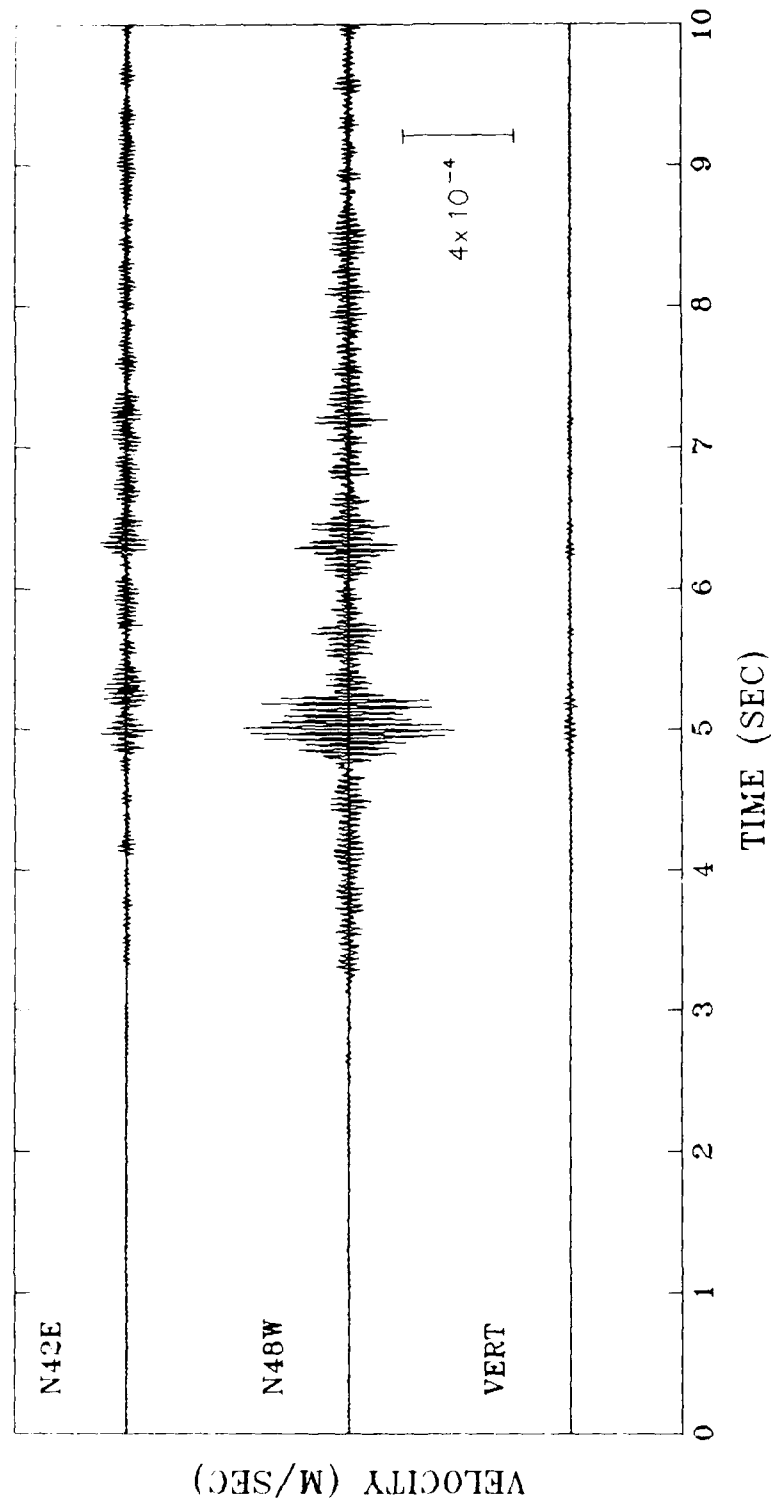


Figure 14. Long Wall Segment Maximum Response for RF-4C Overflight 3

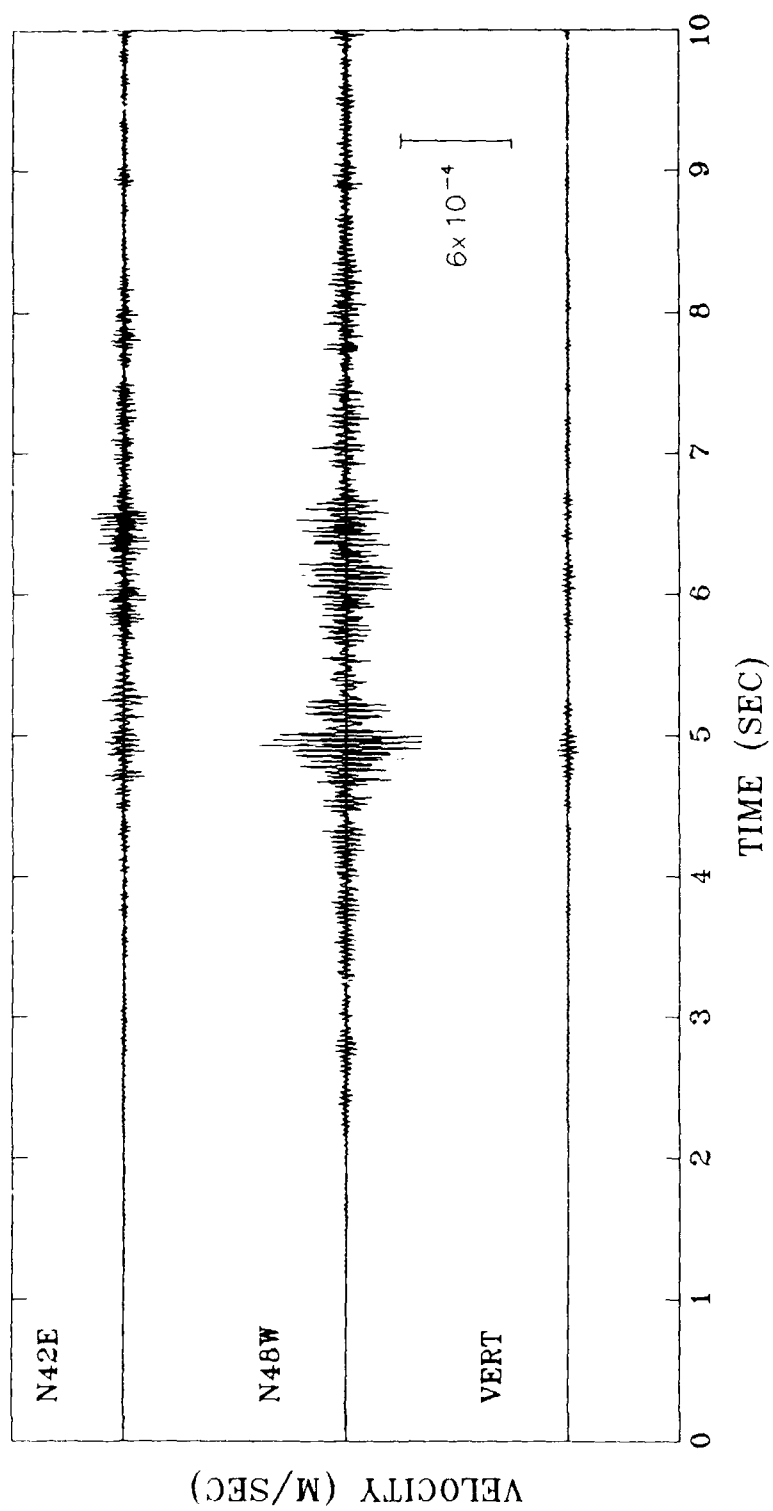


Figure 15. Short Wall Maximum Response for RF-4C Overflight 5

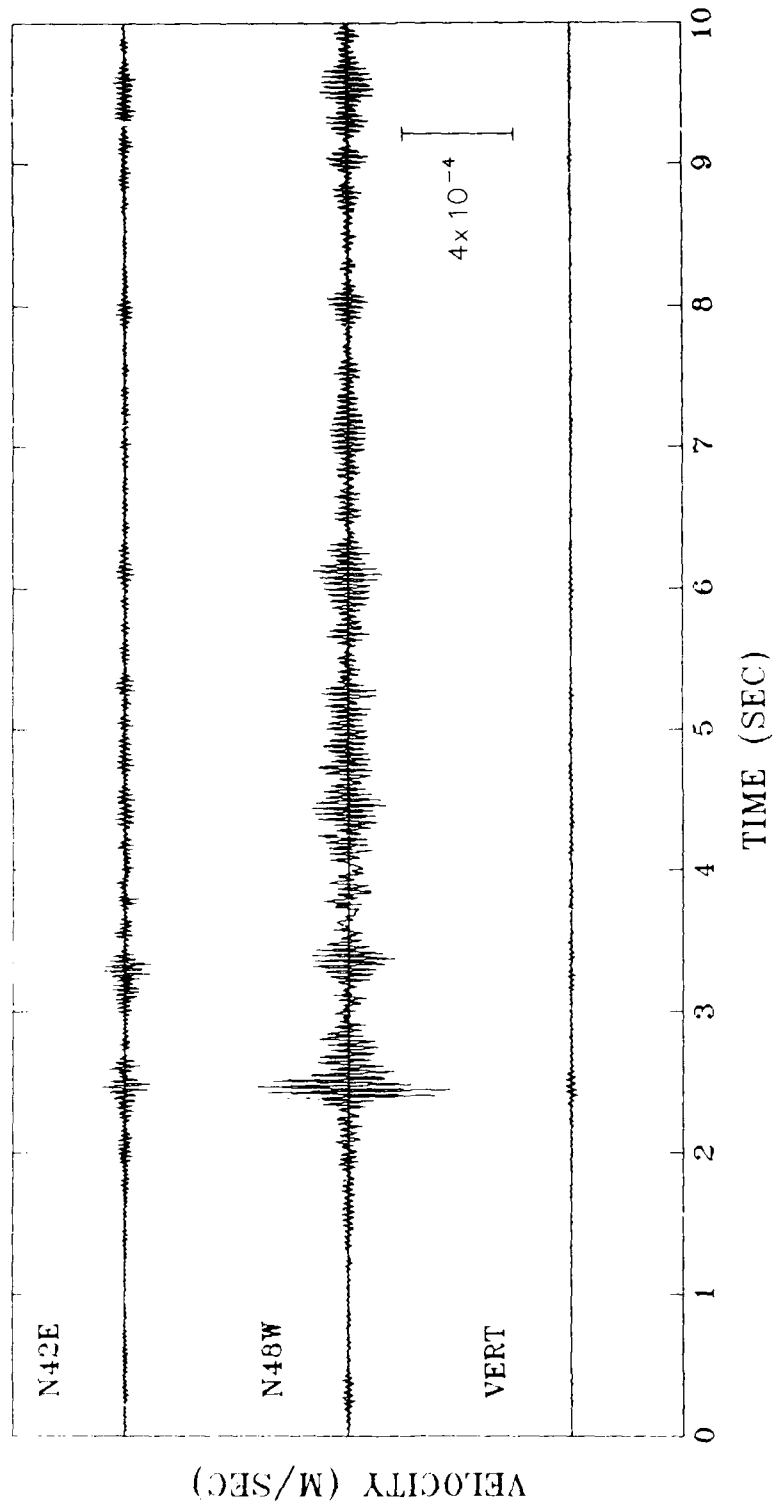


Figure 16. Long Wall Segment Maximum Response for A-7 Overflight 9

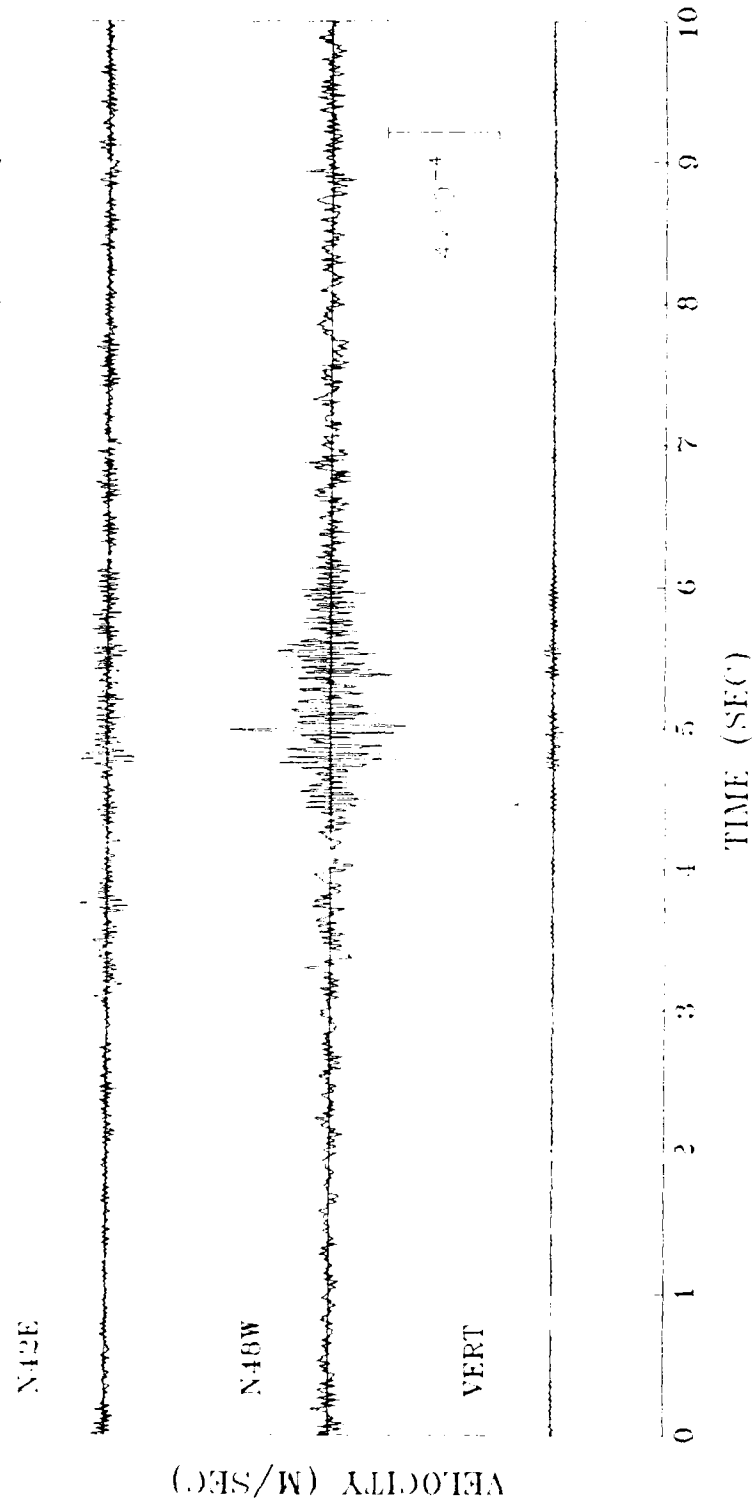


Figure 17. Short Wall Maximum Response for A-7 Overflight 16

Of note in these figures is the temporal asymmetry of the wall responses for RF-4C and A-7 overflights. Although pressure data are not available for corroboration, it appears that maximum wall responses at both sites 2 and 5 occurred just after the aircraft passed overhead and that the wall motions tend to persist much longer than they precede the aircraft. This suggests that acoustics from the jet exhausts were the dominant wall loads during small aircraft passes.

Figures 18 through 21 show the maximum entropy spectral estimates for the time of maximum wall response during the RF-4C and A-7 overflights at each site. Spectral estimates for both types of aircraft at site 2, the long wall segment, are very similar in terms of the peak response frequencies to the estimates obtained for B-52 overflights at this site, as shown in Figure 12. During the A-7 overflight, there is an indication of resonance occurring near 11 Hz that had not previously been observed. The response characteristics for site 5, Figures 13, 19, and 21 for the B-52, RF-4C, and A-7, respectively, appear to be less stable but are in general agreement. The variability of response at site 5 appears to result from the reduced bonding of the upper wall blocks due to erosion of the mortar joints and, in turn, the higher degrees of freedom as compared to site 3.

## **7. WALL ADMITTANCES**

For a linear elastic system, the relationship between a given pressure loading function, defining the time and spatial distribution of the load and the motion response of some site to that load is known as the admittance function and is independent of the amplitude of the load. Given this function, estimates of the response of the system to a similar class of load but of different spectral content can readily be attained. Conversely, if two sites can be shown to have "similar" admittance functions, then it can be shown that the response to a similar event, such as a B-52 overflight, will be similar. The admittance function can be used to classify sites for estimation of overflight responses.

### **7.1 Overflight Admittances**

Based on the B-52 overflights, wall admittances were estimated for the long and short wall segments at Long House. The admittance functions were established by forming the ratio of the square root of the power spectral density functions for the wall motion and the pressure field for a window around the time of peak wall response. The admittances formed for each overflight were then averaged over all passes to give the final estimate. These functions are displayed in Figures 22 and 23 for both the component normal to the axis of the walls, N48W, and parallel to the axis, N42E.

Due to the averaging process used to generate the functions, the resonant modes appear less well defined in these figures. While some scatter in the estimated admittance function is evident between overflights, as would be expected for any form of spectral estimate, the admittance functions for both wall segments appear to be reasonably stable. The admittance functions do not indicate a strong dependence of wall response on the azimuth of approach of the aircraft. It had been anticipated that some change in the admittance would be noted for passes running parallel to the wall axis versus normal to the axis. Apparently the randomness of the aircraft acoustics and the relatively short lengths of the wall segments obscured the anticipated effect.

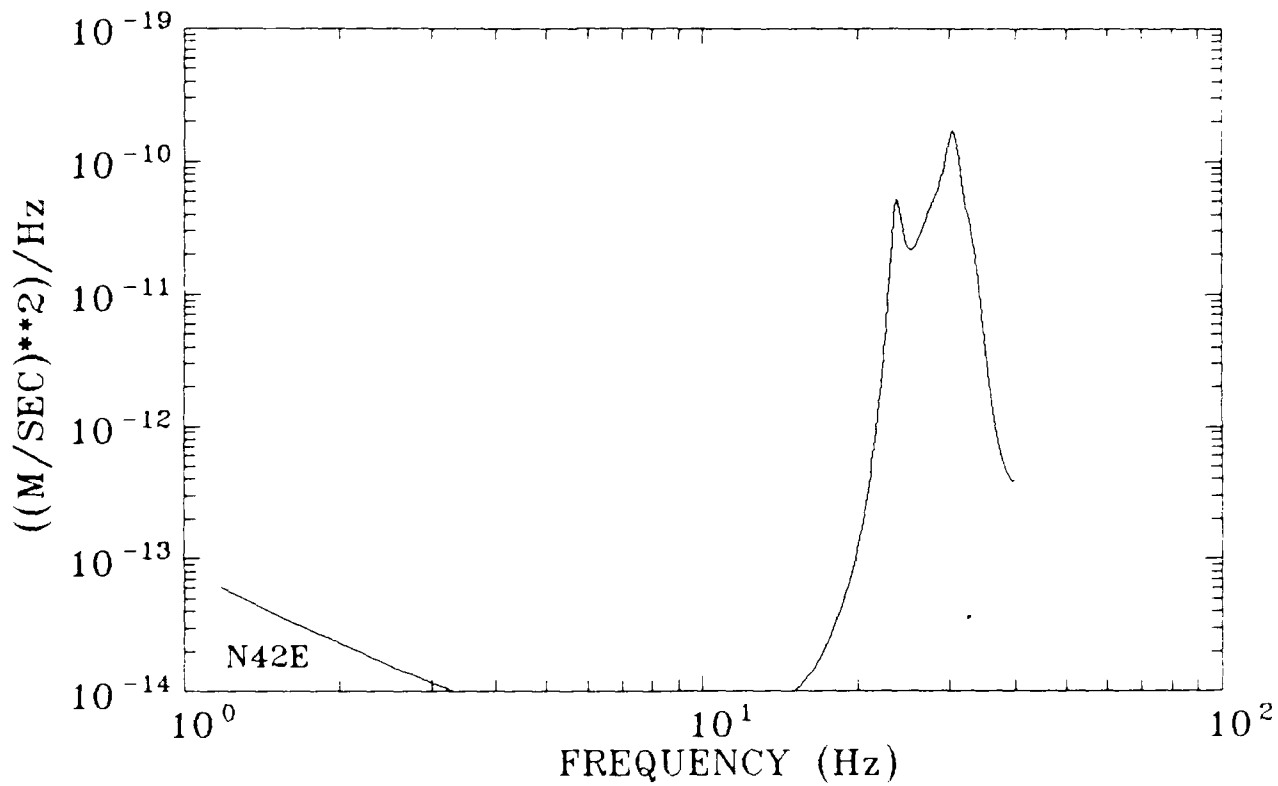


Figure 18a. Maximum Entropy Spectral Estimates of the Wall Motions at Site 2, the Long Wall Segment, During RF-4C Overflight 3. Components of motion are N42E.



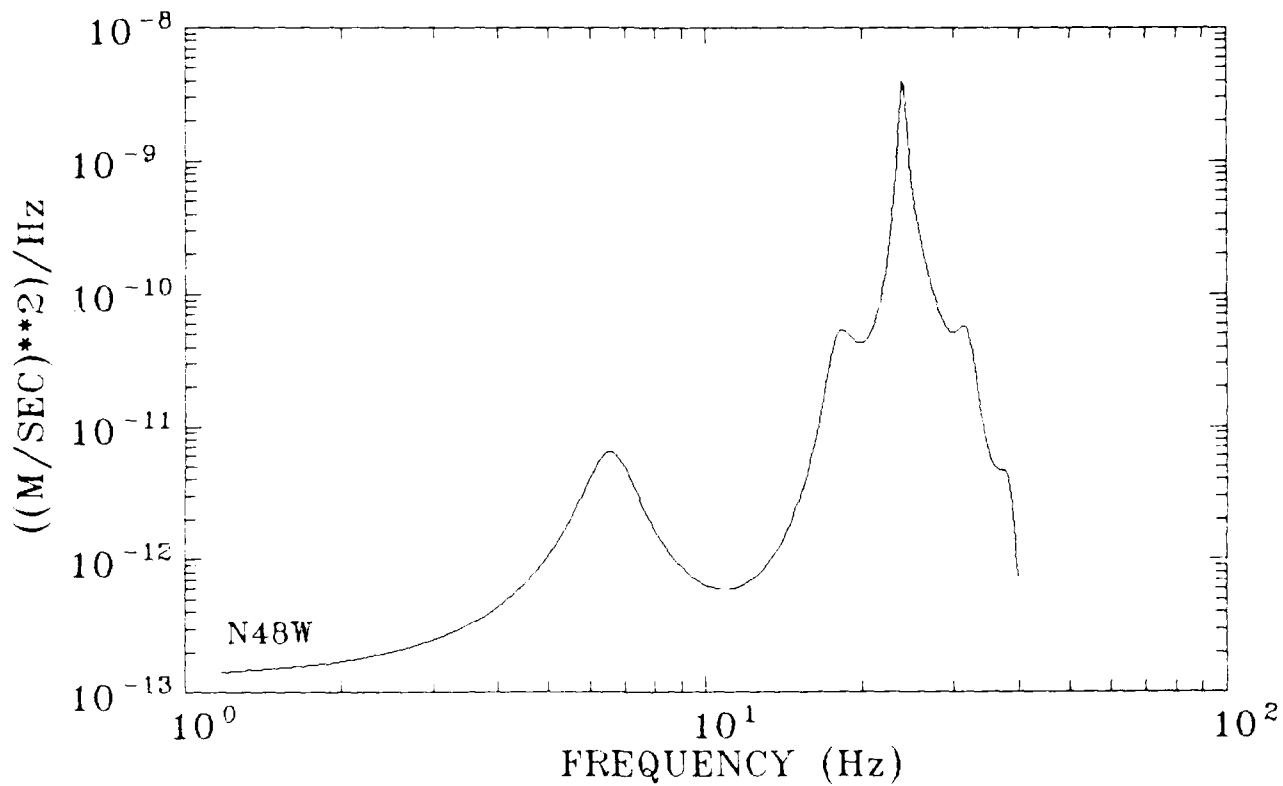


Figure 18b. Maximum Entropy Spectral Estimates of the Wall Motions at Site 2, the Long Wall Segment, During RF-4C Overflight 3. Components of motion are N48W.

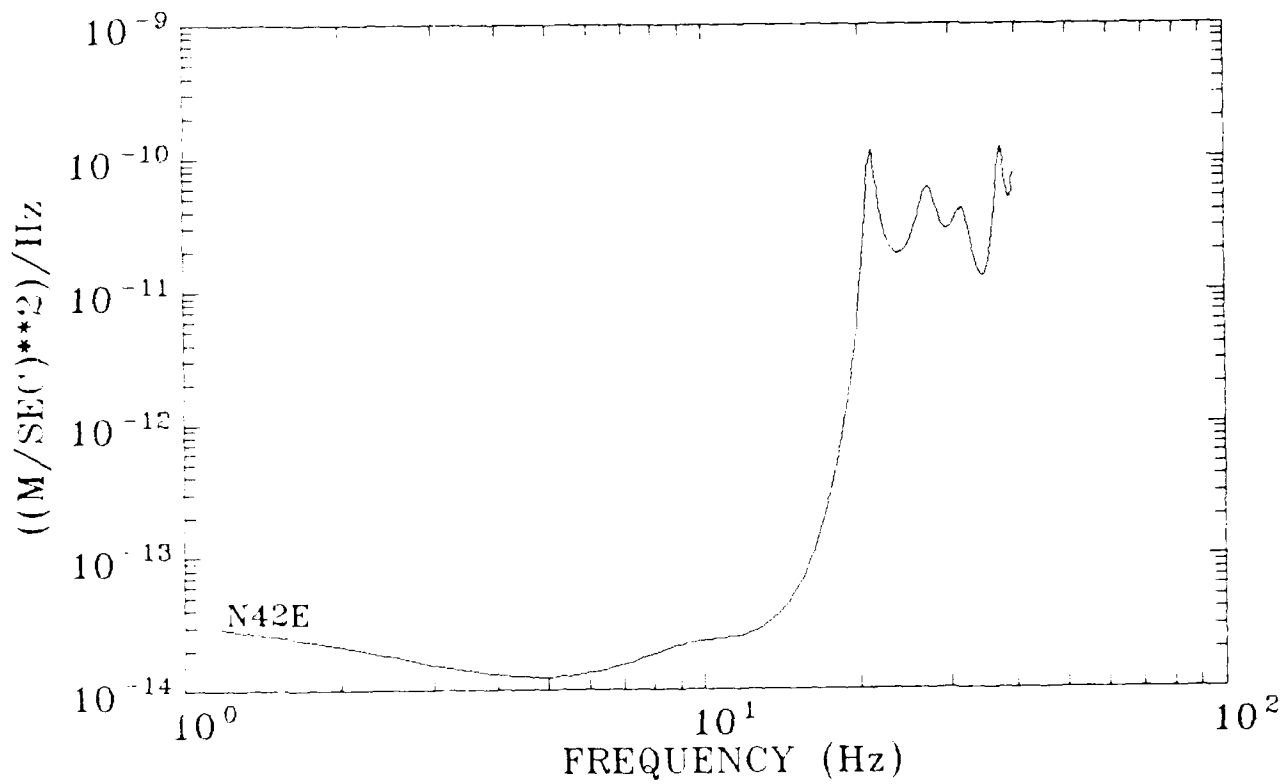


Figure 19a. Maximum Entropy Spectral Estimates of the Wall Motions at Site 5, the Short Wall Segment, During RF-4C Overflight 5. Components of motion are N42E.

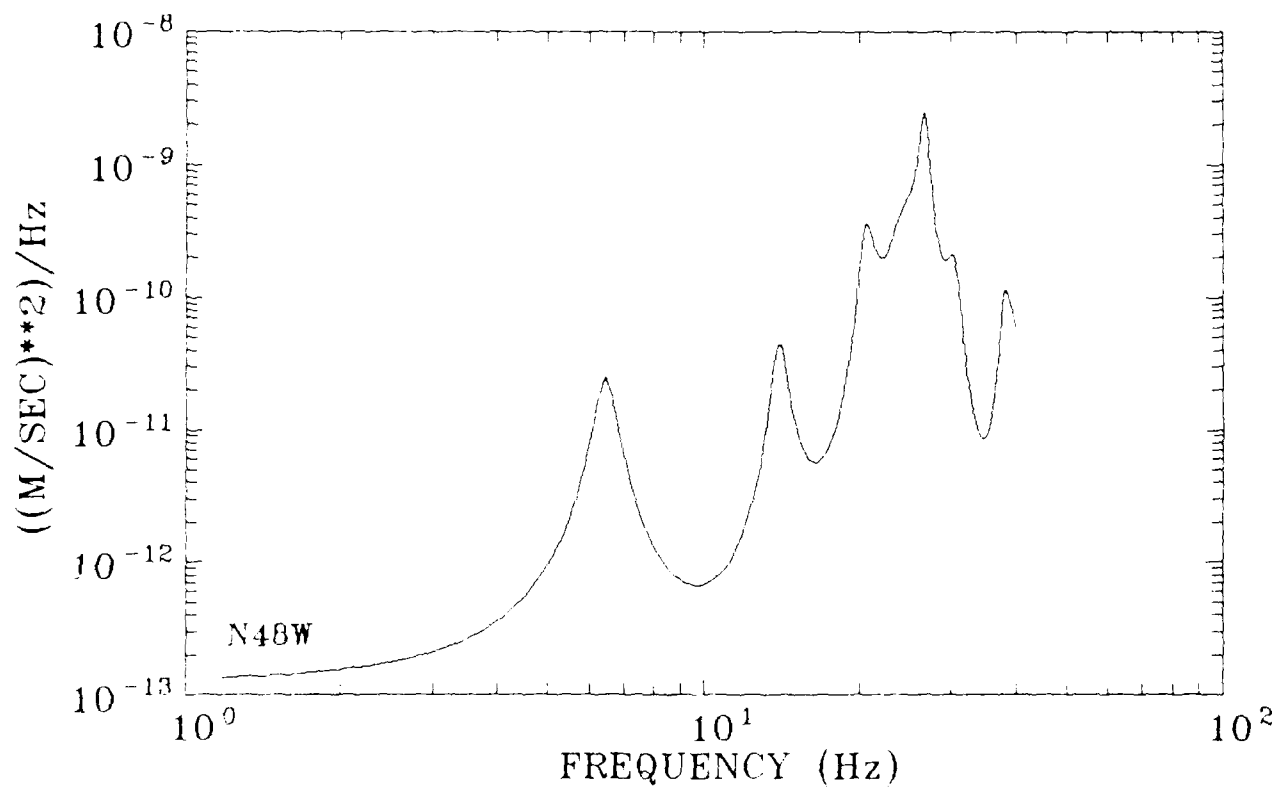


Figure 19b. Maximum Entropy Spectral Estimates of the Wall Motions at Site 5, the Short Wall Segment, During RF-4C Overflight 5. Components of motion are N48W.

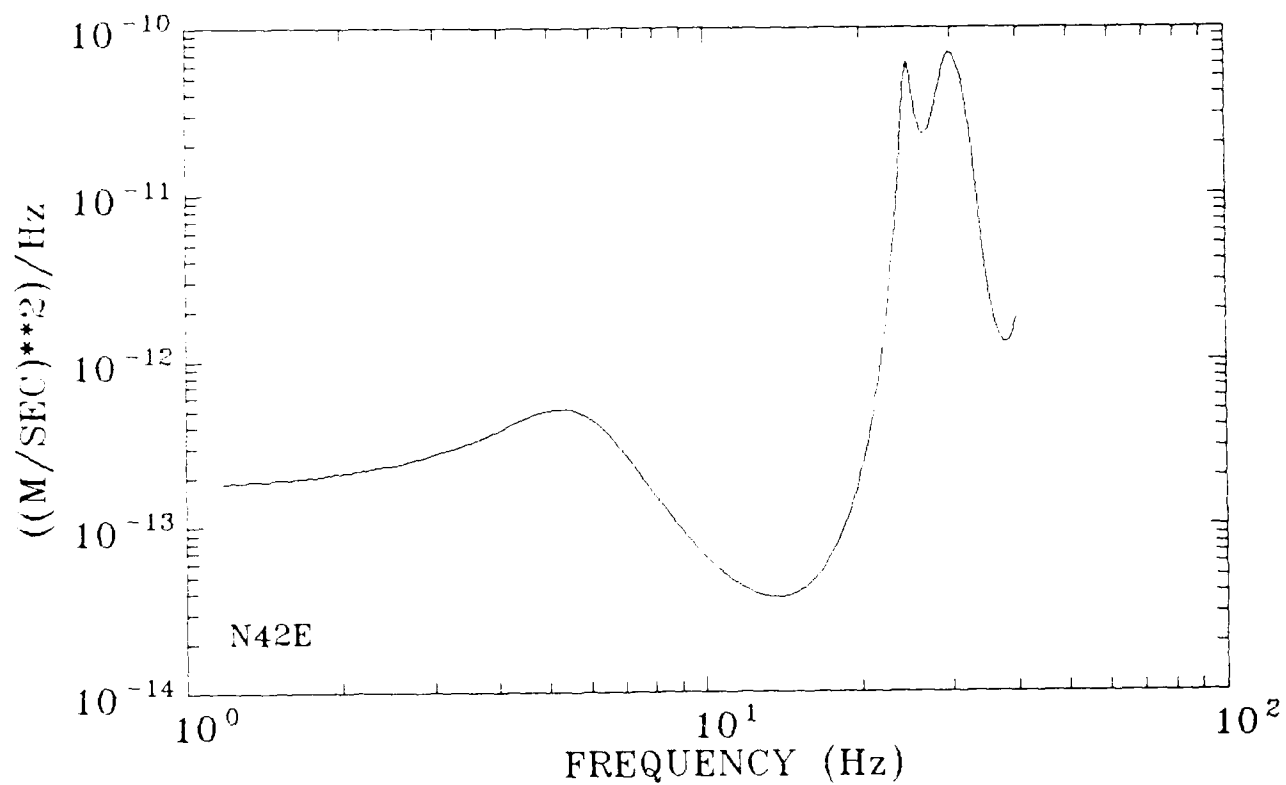


Figure 20a. Maximum Entropy Spectral Estimates of the Wall Motions at Site 2, the Long Wall Segment, During A-7 Overflight 9. Components of motion are N42E.

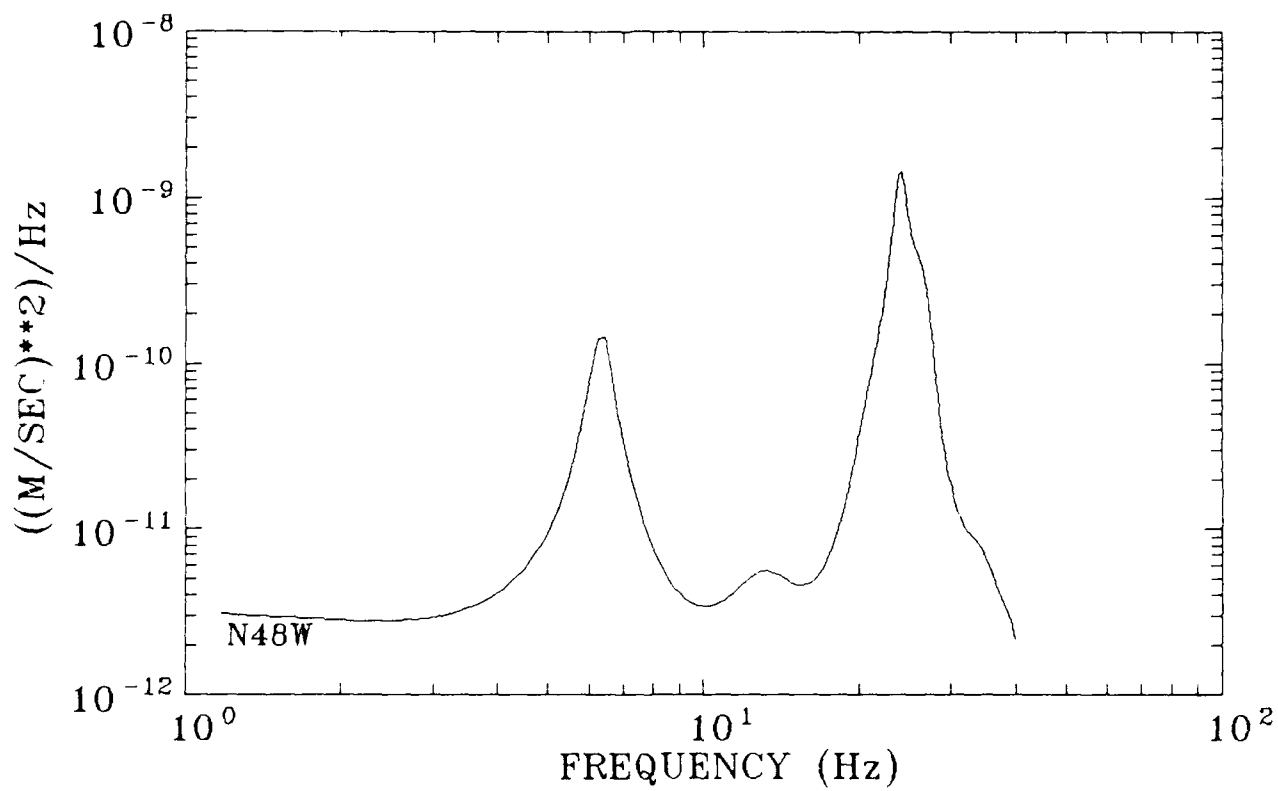


Figure 20b. Maximum Entropy Spectral Estimates of the Wall Motions at Site 2, the Long Wall Segment, During A-7 Overflight 9. Components of motion are N48W.

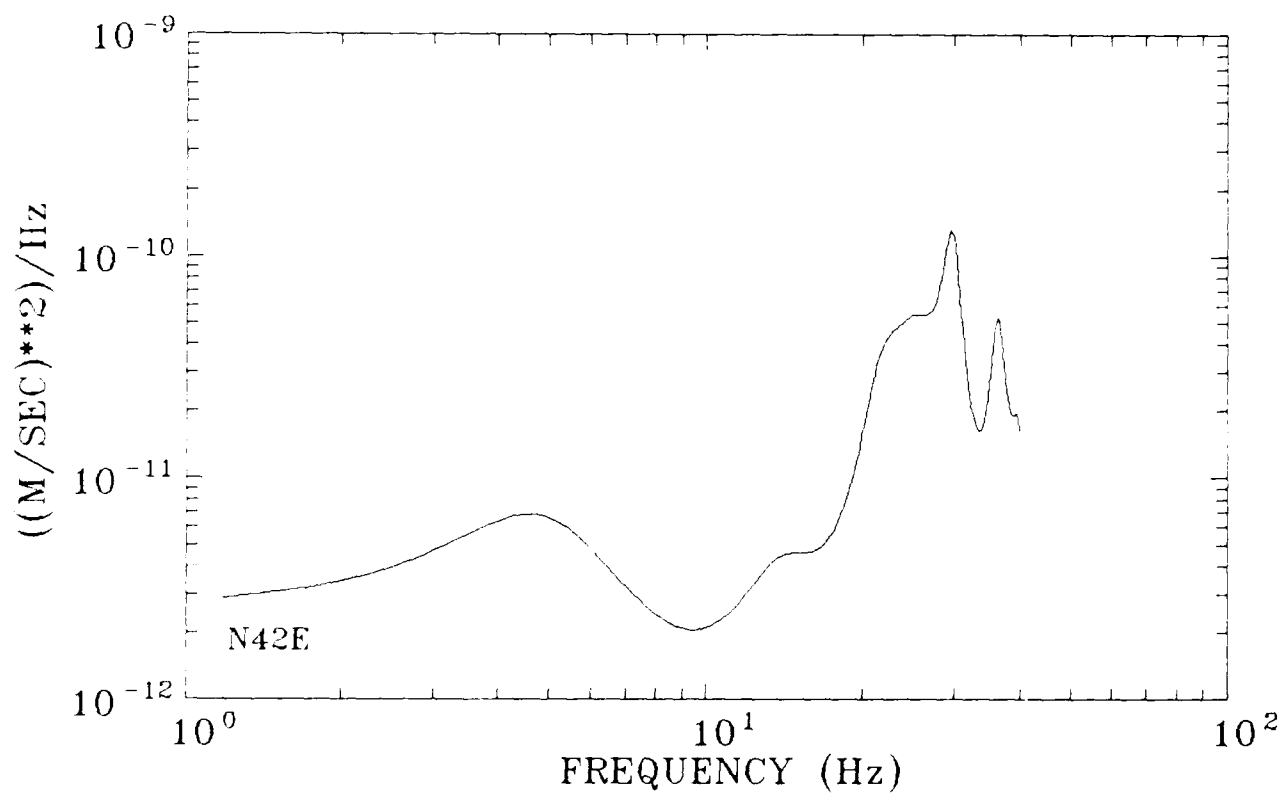


Figure 21a. Maximum Entropy Spectral Estimates of the Wall Motions at Site 5, the Short Wall Segment, During A-7 Overflight 16. Components of motion are N42E.

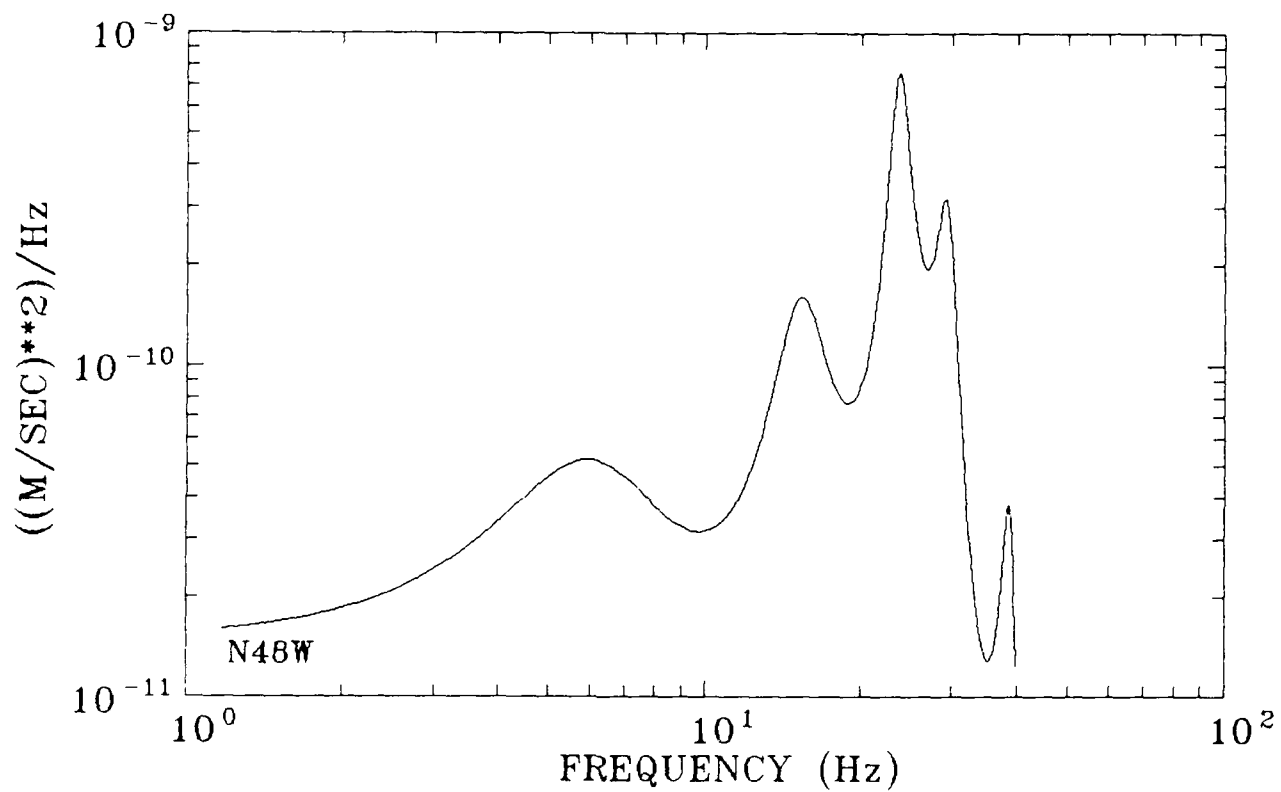


Figure 21b. Maximum Entropy Spectral Estimates of the Wall Motions at Site 5, the Short Wall Segment, During A-7 Overflight 16. Components of motion are N48W.

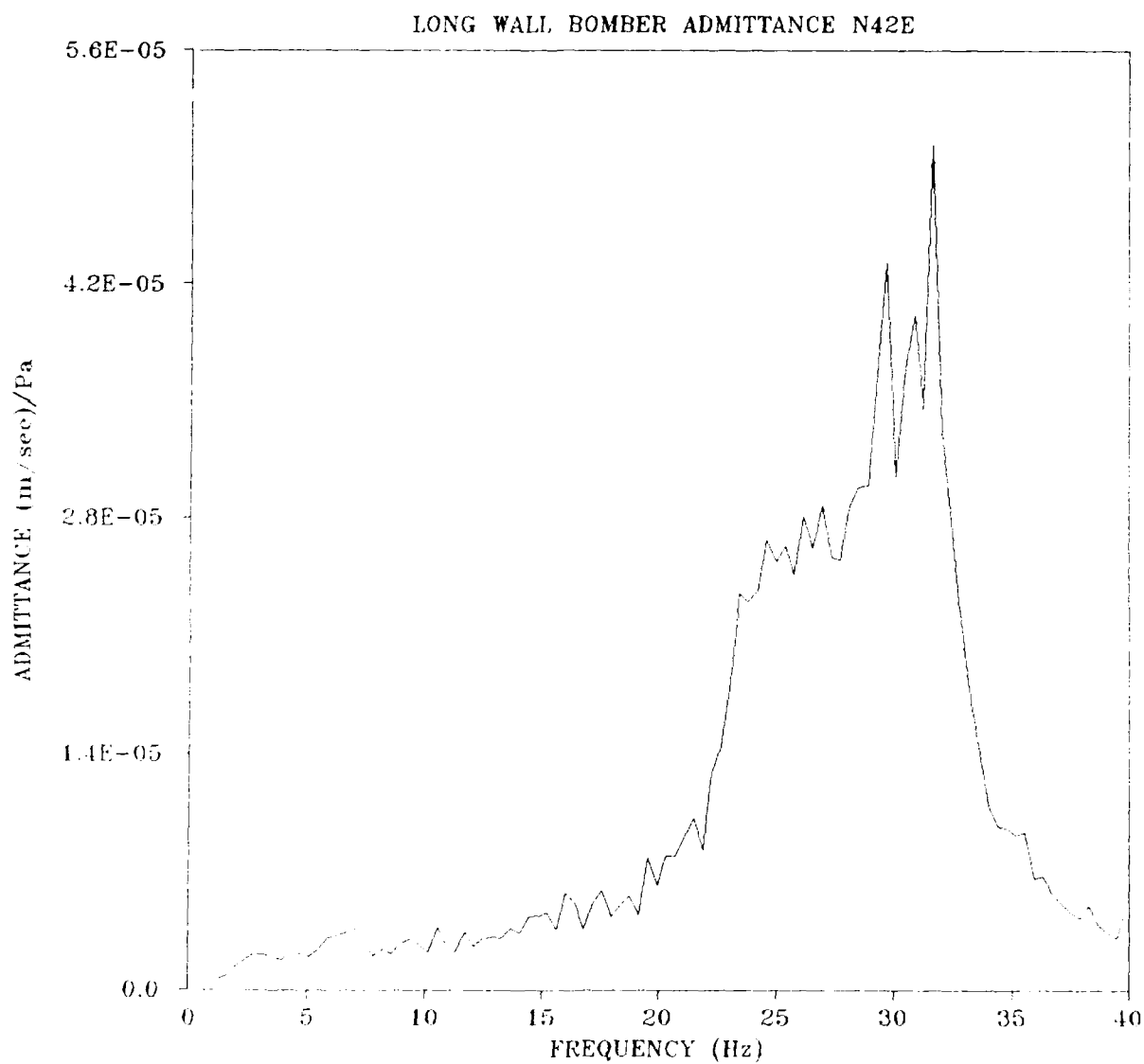


Figure 22a. Long Wall Segment Admittance Function Based on B-52 Overflight Data. Components of motion are N42E.



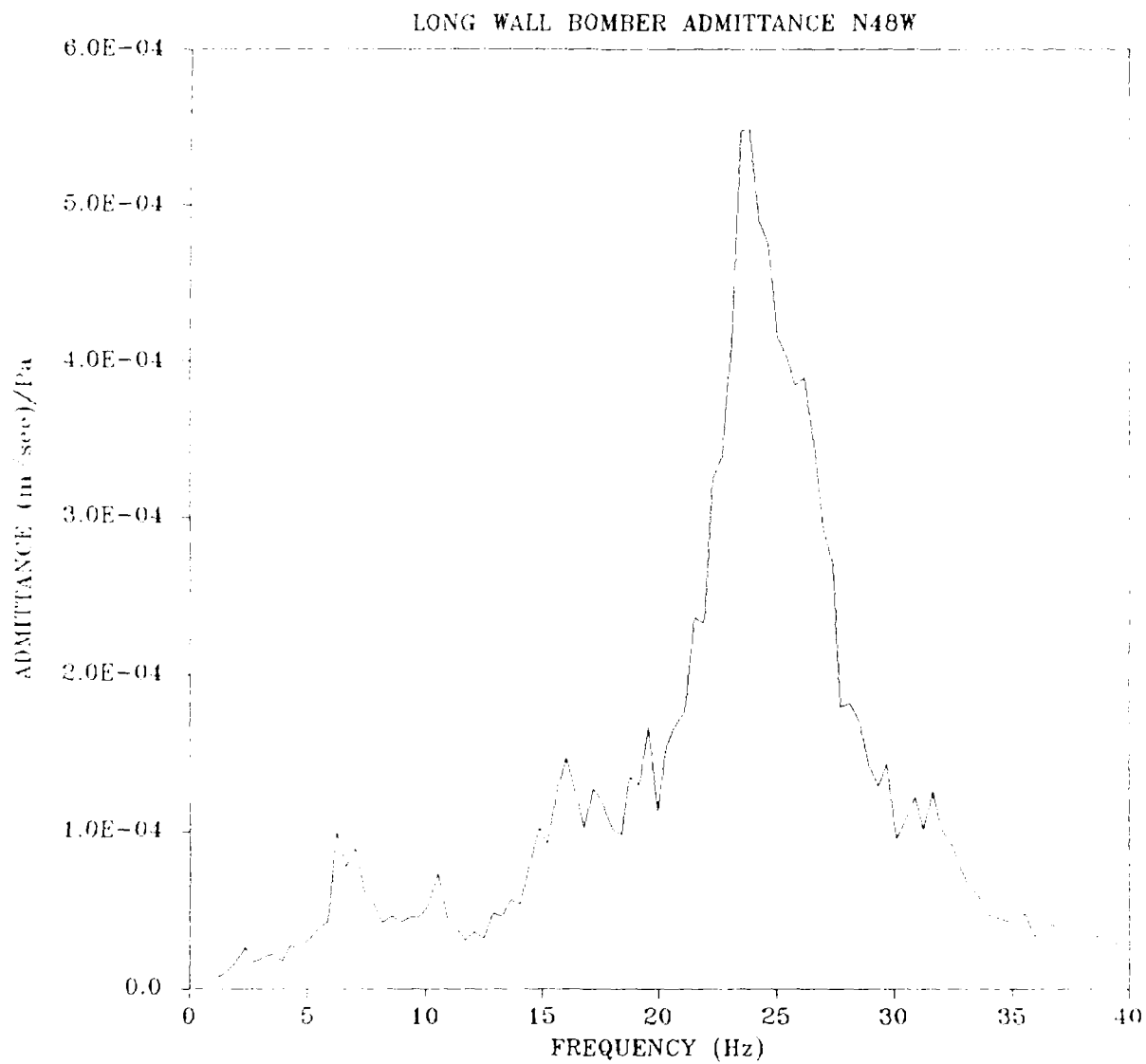


Figure 22b. Long Wall Segment Admittance Function Based on B-52 Overflight Data. Components of motion are N48W.

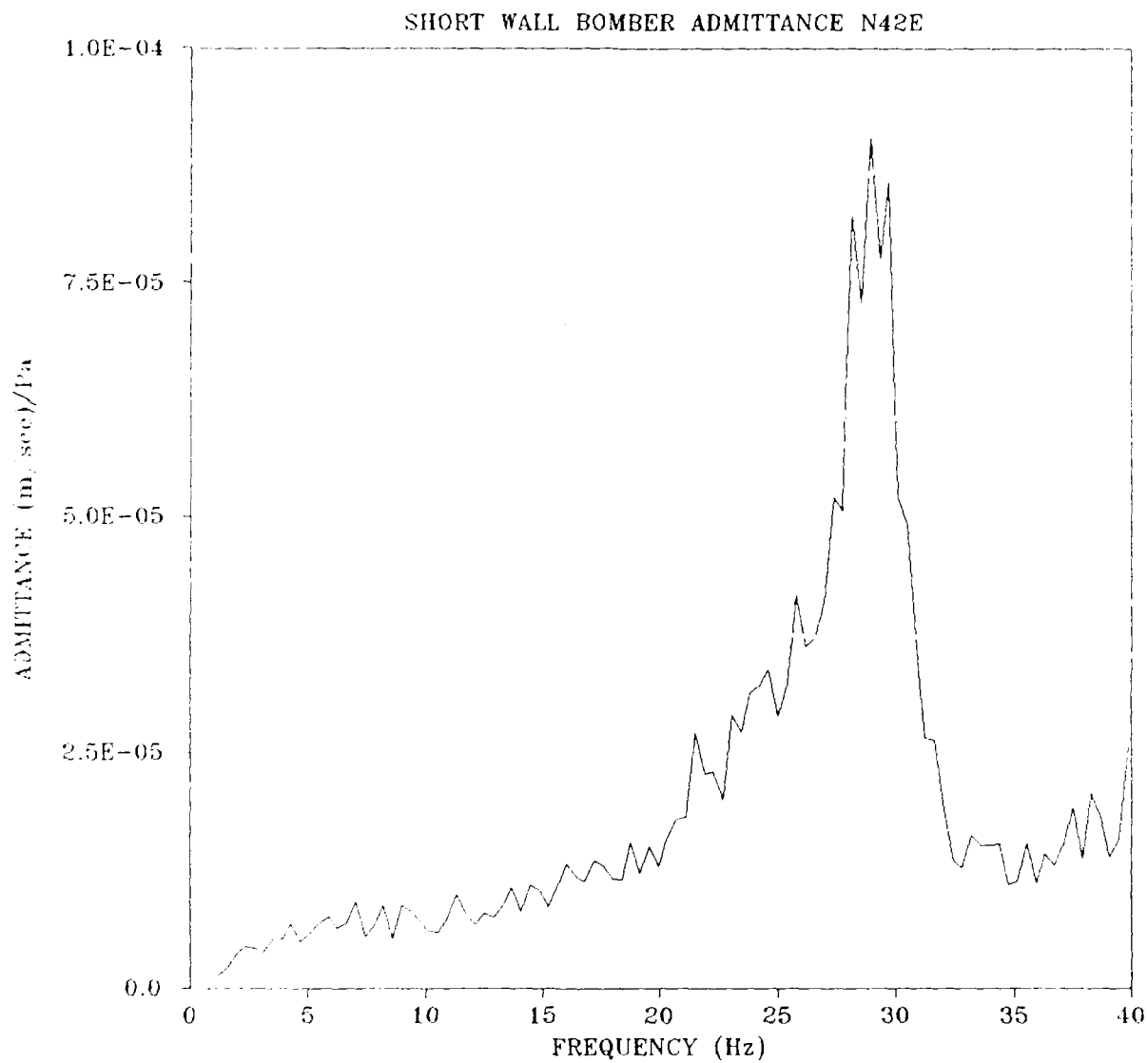


Figure 23a. Short Wall Segment Admittance Function Based on B-52 Overflight Data. Components of motion are N42E.

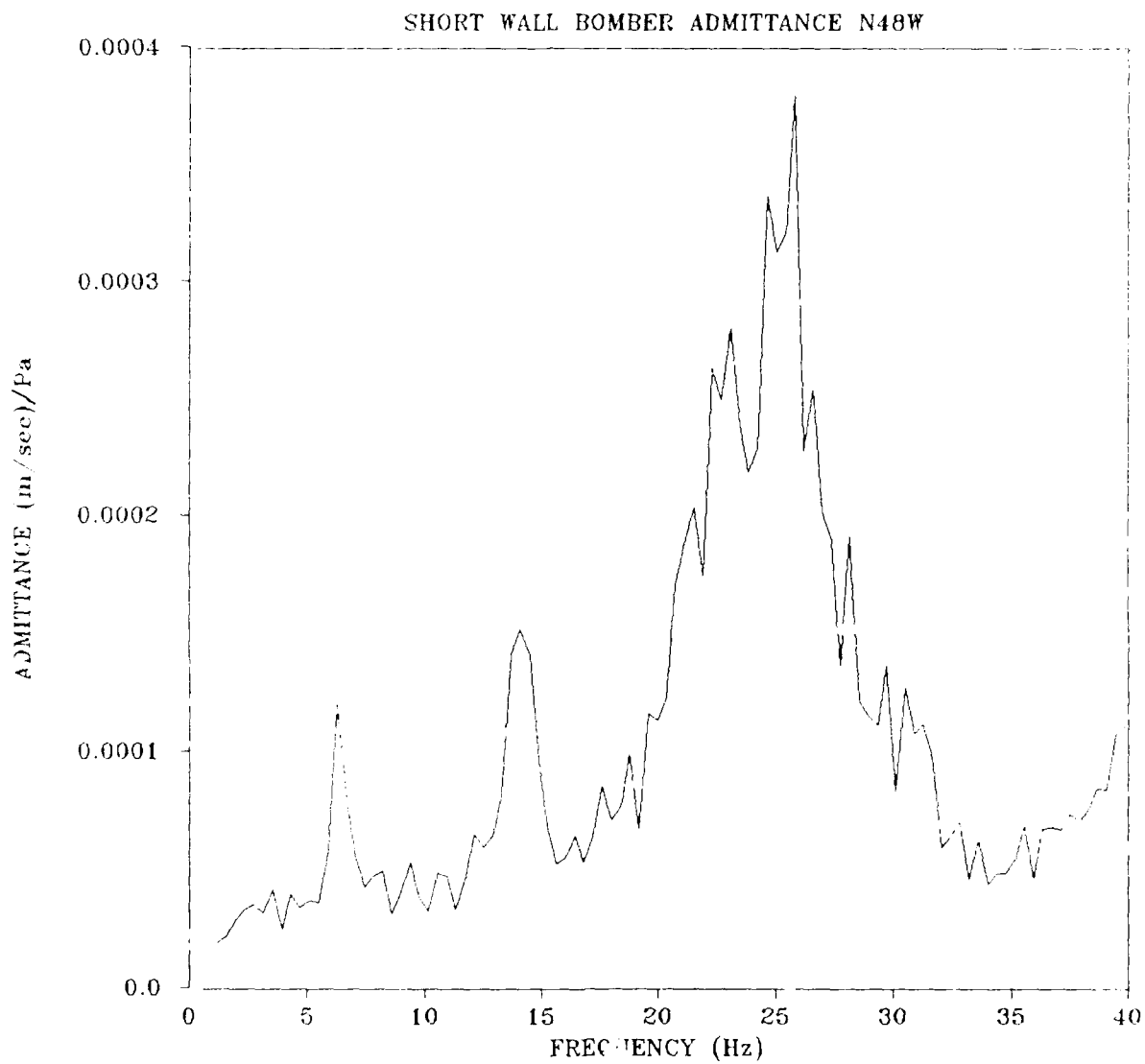


Figure 23b. Short Wall Segment Admittance Function Based on B-52 Overflight Data. Components of motion are N48W.

## 7.2 Shotgun Admittances

In addition to the admittances estimated directly from the overflight data, an attempt was made to estimate wall admittances using the acoustic loads generated by the discharge of blank shotgun shells. If successful, the method could be used as a cost effective means to estimate the response of any given site to aircraft overflights.

Figure 24 shows the estimated admittances for the long wall segment site based on this method. It is apparent that the resonant frequencies of the wall are well defined by this method. However, the admittance functions are significantly lower, by a factor of 10 to 30, than those estimated using the overflight data. Shotgun admittances for the short wall segment are also lower than those based on the overflight data but by a smaller factor.

It appears that the area of the wall with significant loading from the shotgun blast is insufficient to adequately model the response to pressure loads being exerted over the entire wall surface as occurs during overflights. As the total area of the wall decreases, however, the shotgun blast based admittances should converge with the overflight admittances. It can be concluded that shotgun blasts are insufficient for admittance estimation for large, massive walls. However, the method, with further development, might still be applicable for less massive structures.

## 8. RESULT SUMMARY

The induced motions of two wall segments at Long House, an Anasazi Indian site in northeastern Arizona, were monitored during low altitude overflights of B-52, RF-4C, and A-7 aircraft. The motion levels observed during all passes were well below established criteria for vibration in ancient structures, a level of 1.3 mm/sec. The B-52 overflights were conducted at a range of altitudes and speeds typical for low level training missions. Several of the RF-4C and A-7 passes could be characterized as intense and likely representing the most extreme overflight conditions of low altitude and high air speed. For Long House and similar sites, it can be concluded that aircraft overflights within the bounds of the measured passes have no significant vibration effect.

The attempt to develop a cost effective method to estimate admittance functions for archaeological sites was considered to be a qualified failure. The acoustic source, a shotgun firing blanks, provided an inadequate pressure load for large, massive walls such as those at Long House, to estimate admittance for aircraft overflights. For smaller, less massive structures, however, there are indications that the technique might be adequate. Further work would be required to establish the adequacy and limits of the technique.

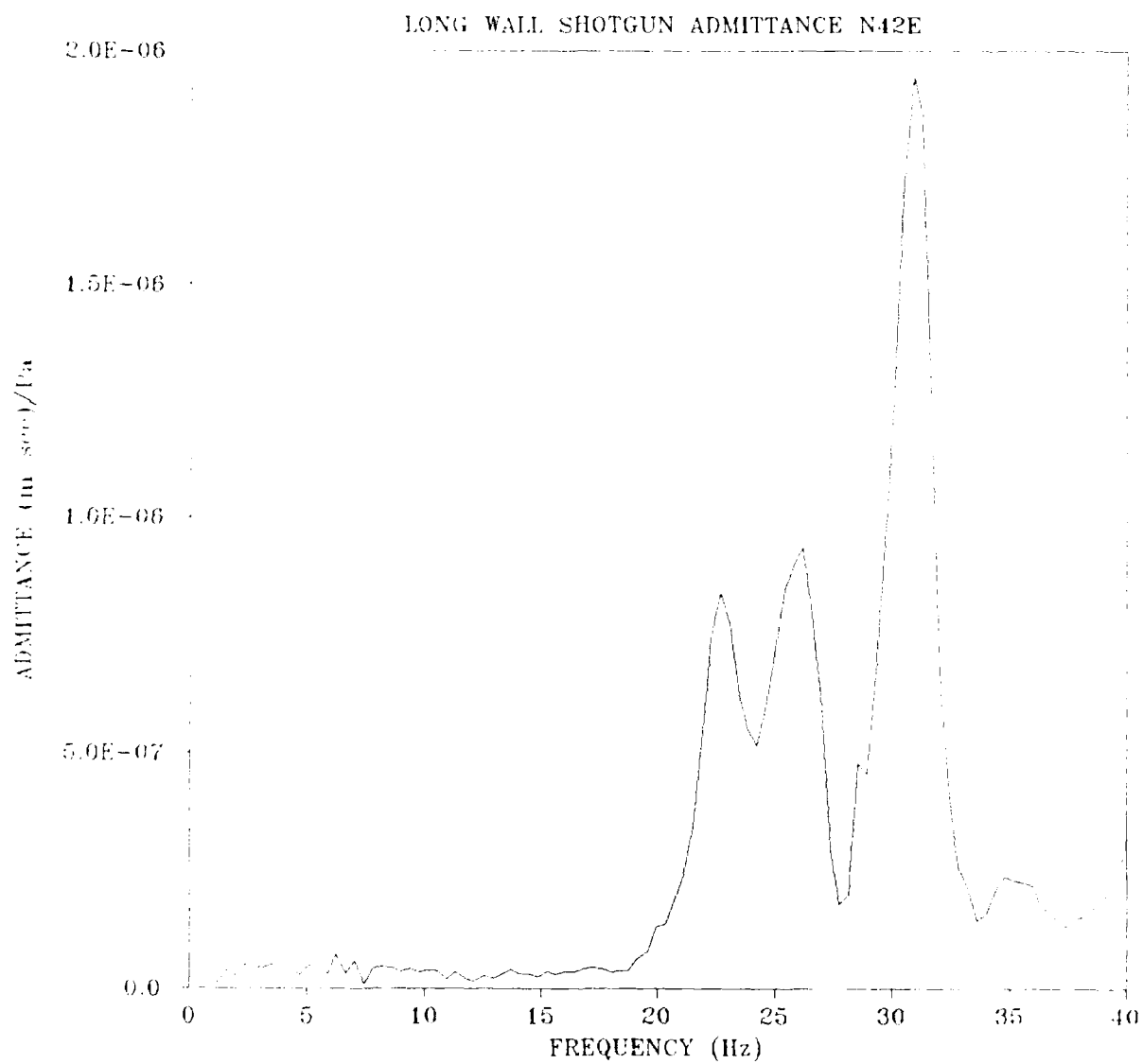


Figure 24a. Long Wall Segment Admittance Function Based on Shotgun Blasts. Components of motion are N42E.

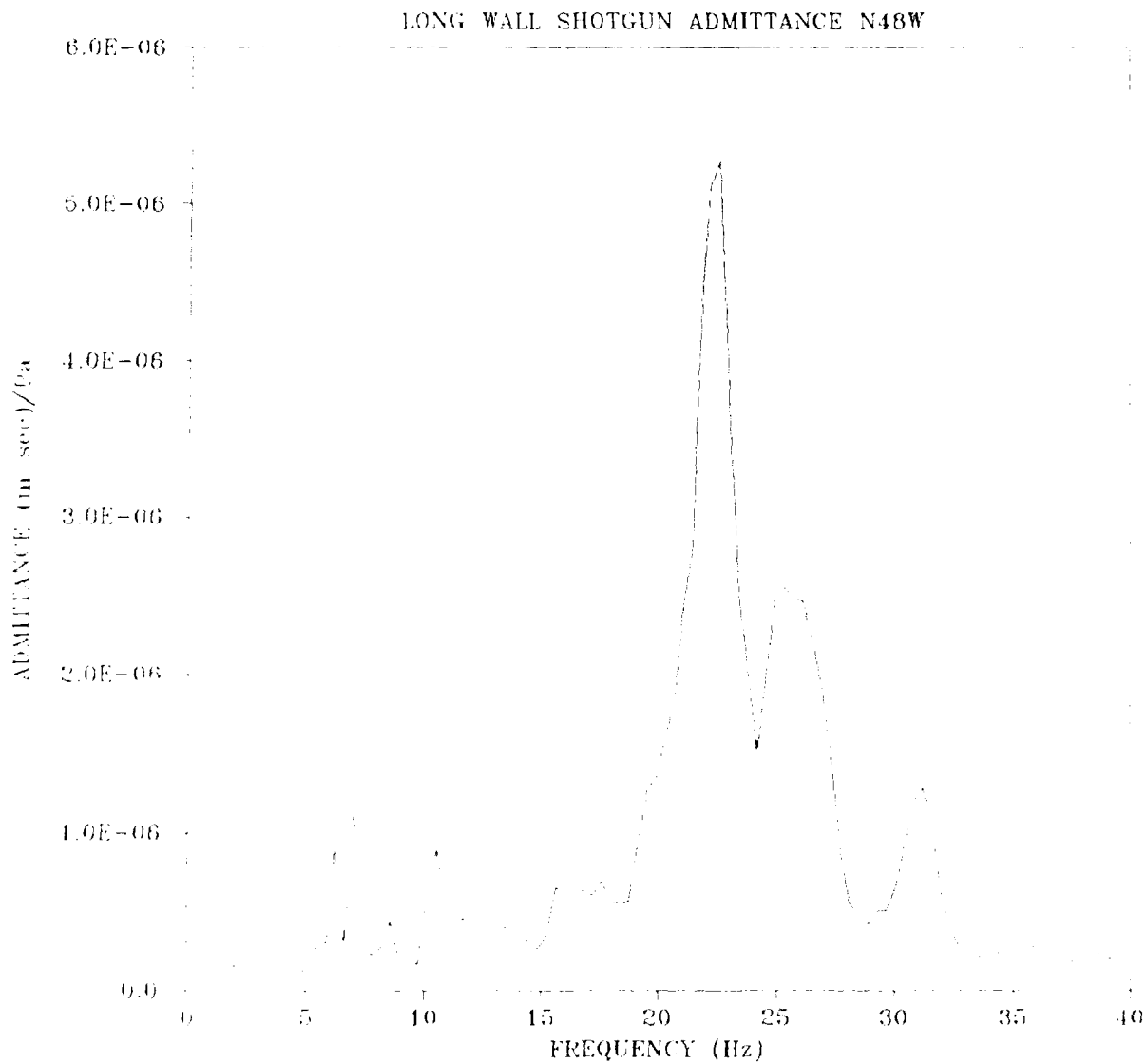


Figure 24b Long Wall Segment Admittance Function Based on Shotgun Blasts. Components of motion are N48W.

## References

1. Dean, J.S. (1969) Chronological Analysis of Tsegi Phase Sites in Northeastern Arizona. *Papers of the Laboratory of Tree-Ring Research*, No. 3, University of Arizona Press.
2. King, W.K., Algermissen, S.T., and McDermott, P.J. (1985) *Seismic and Vibration Hazard Investigation of Chaco Culture National Historic Park*, Open File Report 85-529, U.S. Geological Survey, Denver, CO.
3. Saurenman, H.J., Nelson, J.T., and Wilson, G.P. (1982) *Handbook of Urban Rail Noise and Vibration Control*, DOT Report No. DOT-TSC-UMTA-81-72, Wilson, Thrig & Associates, Oakland, CA.
4. Bruce, R.D. (1971) Field Measurements: Equipment and Techniques, *Noise and Vibration Control*, L.L. Beranek, Ed., McGraw-Hill Book Co., New York.
5. Grieb, H., and Heinig, K. (1986) Noise Emission of Civil and Military Aero-Engines - Sources of Generation and Measures of Attenuation, *Aircraft Noise in a Modern Society*, H.J. Gummlich and H.D. Marohn, NATO Committee on the Challenges of Modern Society Report No. 161, Mittenwald, Germany.
6. Bisgood, P.L., Maltby, R.L., and Dee, F.W. (1971) Some work at the Royal Aircraft Establishment on the behavior of vortex wakes, *Aircraft Wake Turbulence and Its Detection*, J.H. Olsen, A. Goldberg, and M. Rogers, Eds., Plenum Press, New York.
7. Garodz, L.J., Lawrence, D.M., and Miller, N.J. (1976) *Measurement of the Trailing Vortex Systems of Large Transport Aircraft Using Tower Fly-By and Flow Visualization (Summary, Comparison, and Application)*, FAA-RD-75-127, ADA 021305, Atlantic City, N.J.
8. Houghton, E.L., and Carruthers, N.B. (1976) *Wind Forces on Buildings and Structures: An Introduction*, John Wiley & Sons, New York.
9. Champion, K.S.W., Cole, A.E., and Kantor, A.J. (1985) Standard and Reference Atmospheres, *Handbook of Geophysics and the Space Environment*, A.S. Jurse, Ed., Air Force Geophysics Laboratory, AFGL-TR-85-0315, ADA 167000, Hanscom AFB, MA.